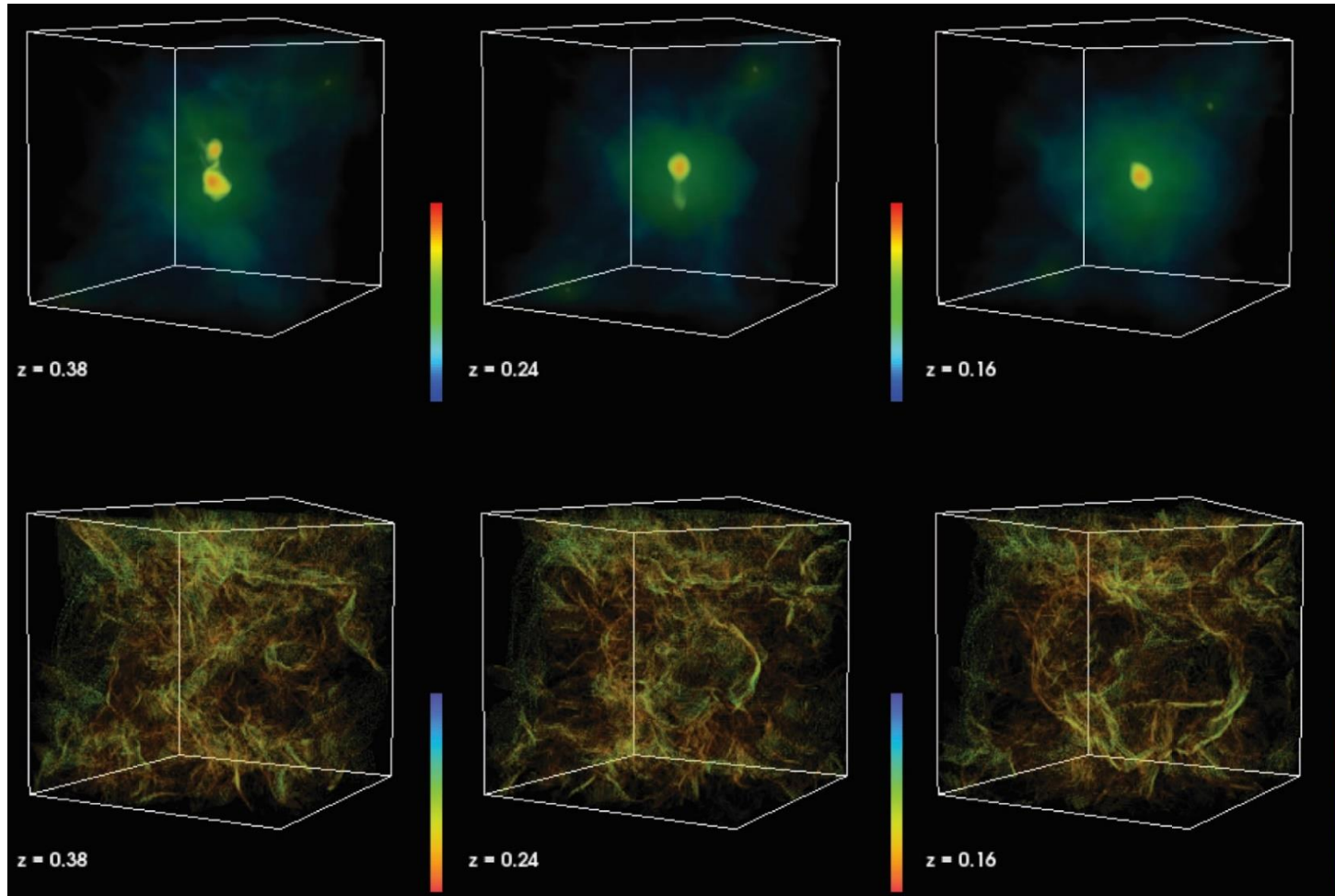


Proton Acceleration at collisionless shocks in galaxy clusters

merging
galaxy
cluster



X-ray

shocks



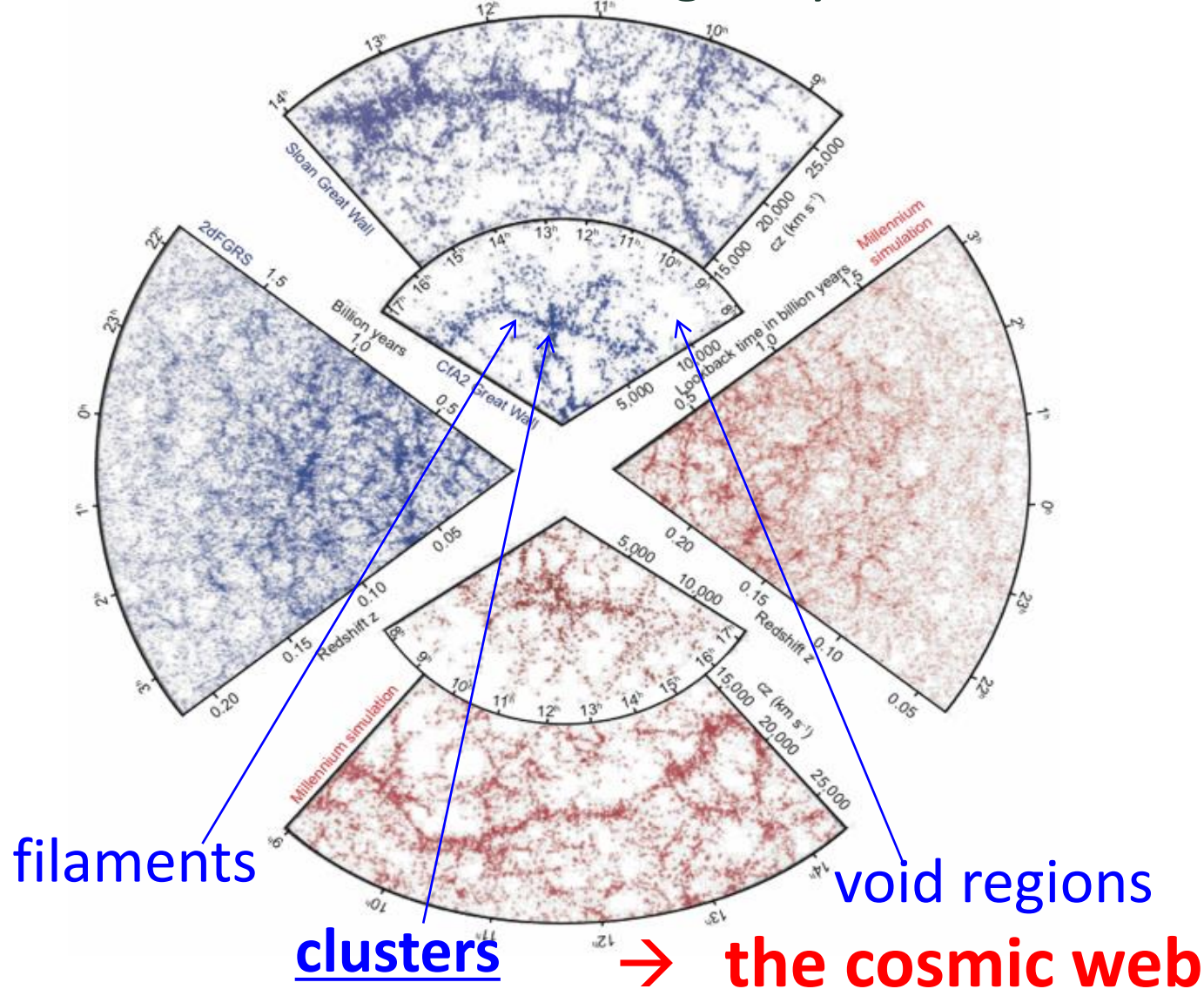
Dongsu Ryu (UNIST, Korea)

Ji-Hoon Ha (UNIST, Korea), Hyesung Kang (Pusan Nat. Univ., Korea)

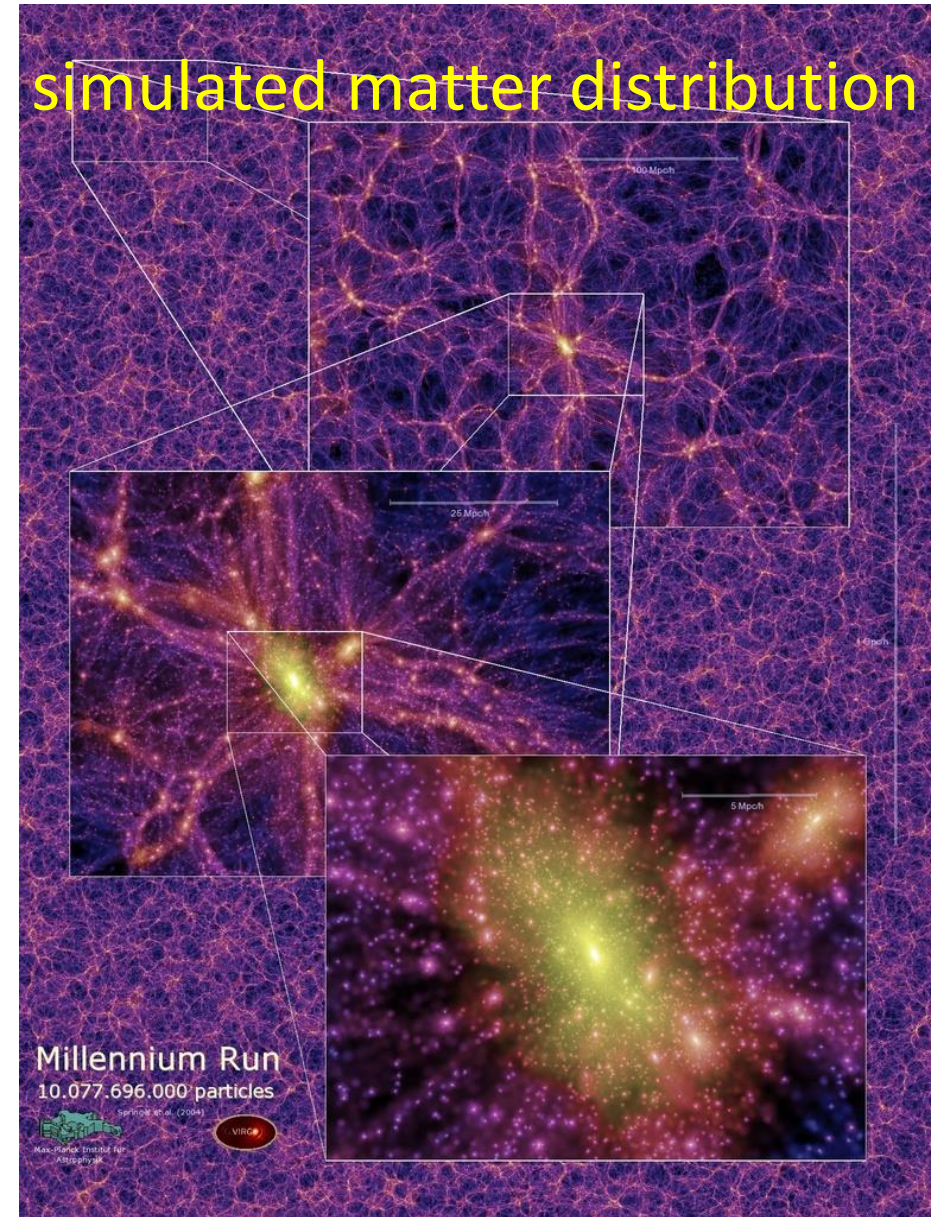


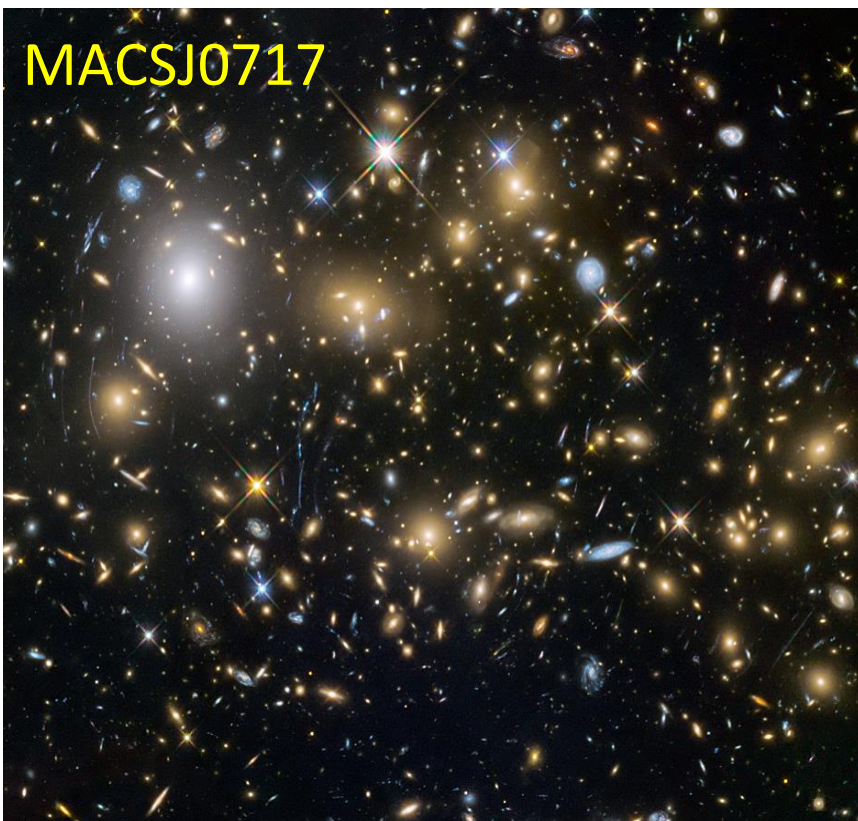
The large-scale structure of the universe

observed and simulated galaxy distribution



simulated matter distribution

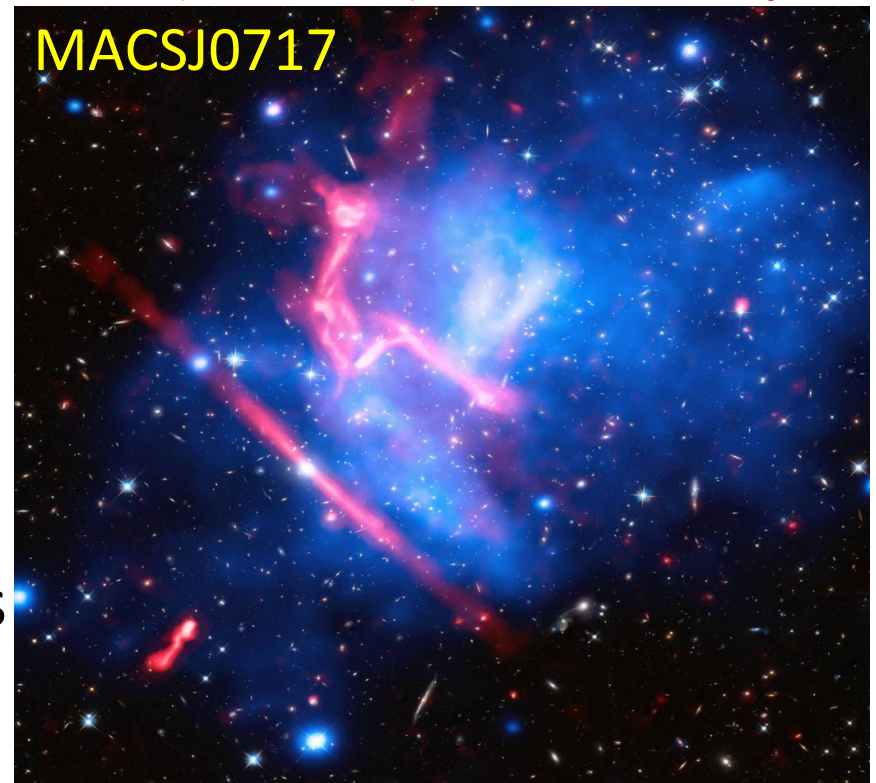




MACSJ0717

Clusters of galaxies: aggregates of galaxies, which are the largest known gravitationally bound objects to have arisen thus far in the process of cosmic structure formation

optical (Hubble, white)
X-ray (Chandra, blue) ← hot gas
radio (VLA, red) ← cosmic rays



MACSJ0717

Hubble space telescope image

The intracluster medium (ICM): the superheated plasma with $T \sim$ a few to several keV, presented in clusters of galaxies

Fluid quantities in the ICM from observations

size of clusters

$$L_{\text{cluster}} \sim \text{a few Mpc} \sim 10^{25} \text{ cm}$$

baryon number density

$$n \sim 10^{-3} \text{ cm}^{-3}$$

gas temperature

$$T \sim 10^8 \text{ K (8.6 keV)} \rightarrow c_s \sim 1,500 \text{ km/s}$$

flow velocity

$$v \sim \text{several} \times 100 \text{ km/s} \rightarrow M_s \sim 1/2 < 1$$

magnetic fields

$$B \sim \text{a few} \times \mu\text{G} \rightarrow c_A \sim 100 \text{ km/s}, M_A > 1$$

→ flows are **subsonic** ($M_s \sim 0.5$) but **super-Alfvénic** ($M_A > 1$)

gas thermal energy

$$\underline{E_{\text{thermal}} \sim \text{a few} \times 10^{-11} \text{ erg/cm}^3}$$

gas kinetic energy

$$\underline{E_{\text{kinetic}} \sim \text{a few} \times 10^{-12} \text{ erg/cm}^3}$$

magnetic energy

$$\underline{E_{\text{magnetic}} \sim \text{a few} \times 10^{-13} \text{ erg/cm}^3}$$

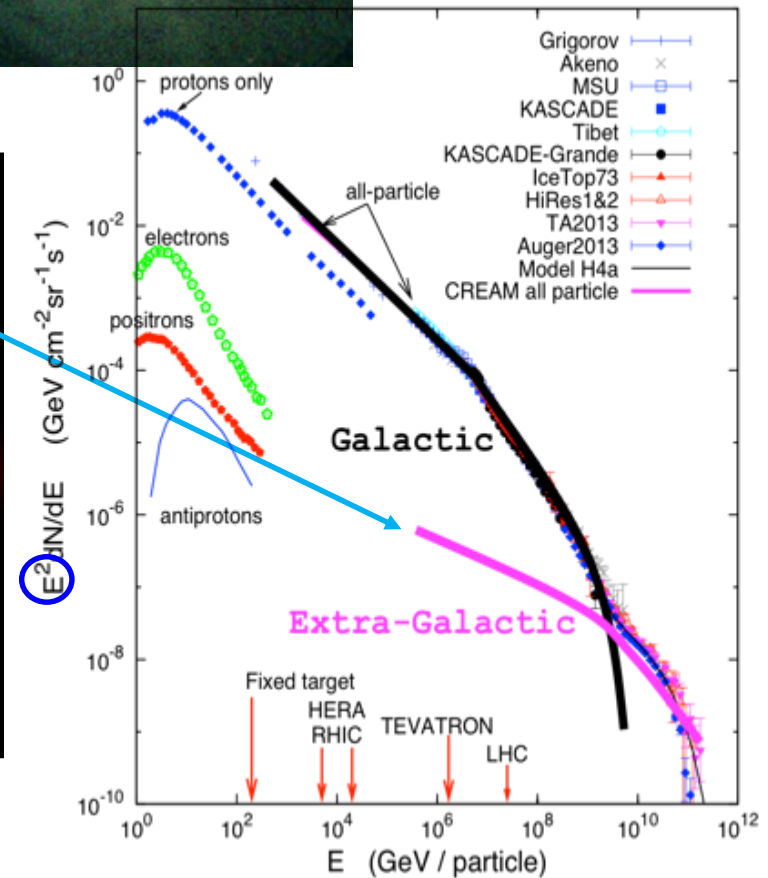
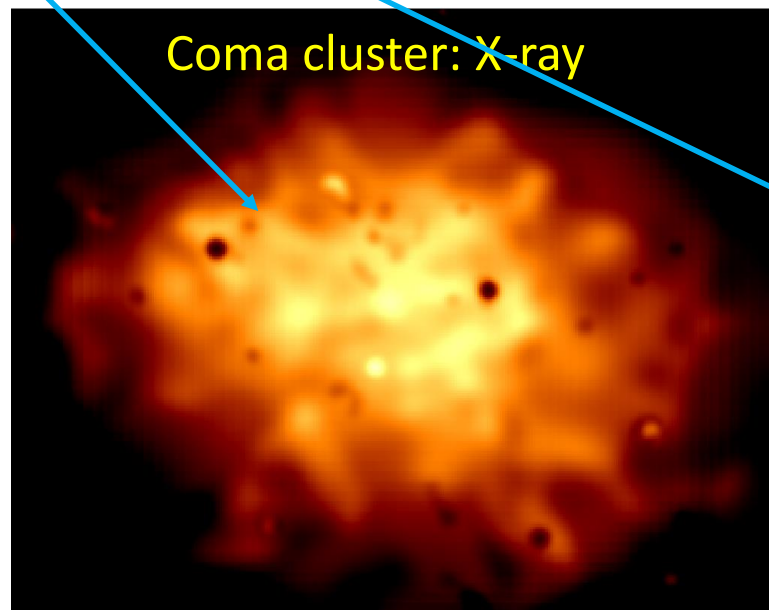
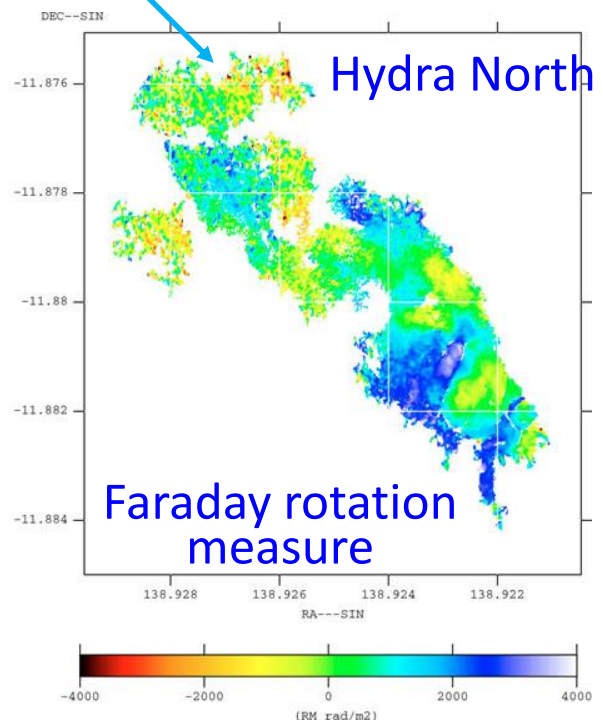
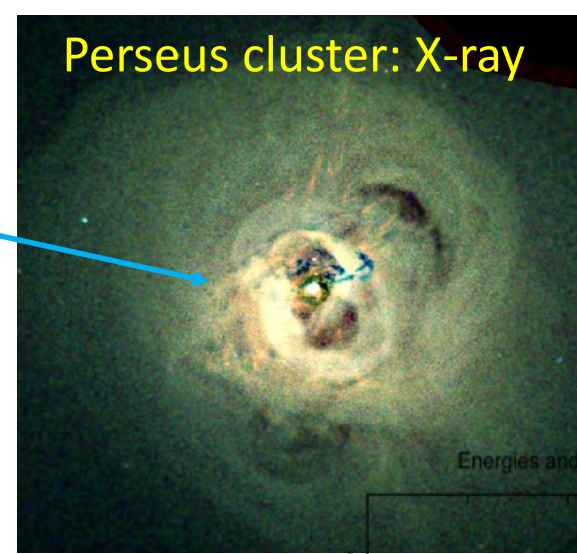
cosmic-ray energy

$$\underline{E_{\text{CR}} < \sim \text{a few} \times 10^{-13} \text{ erg/cm}^3}$$

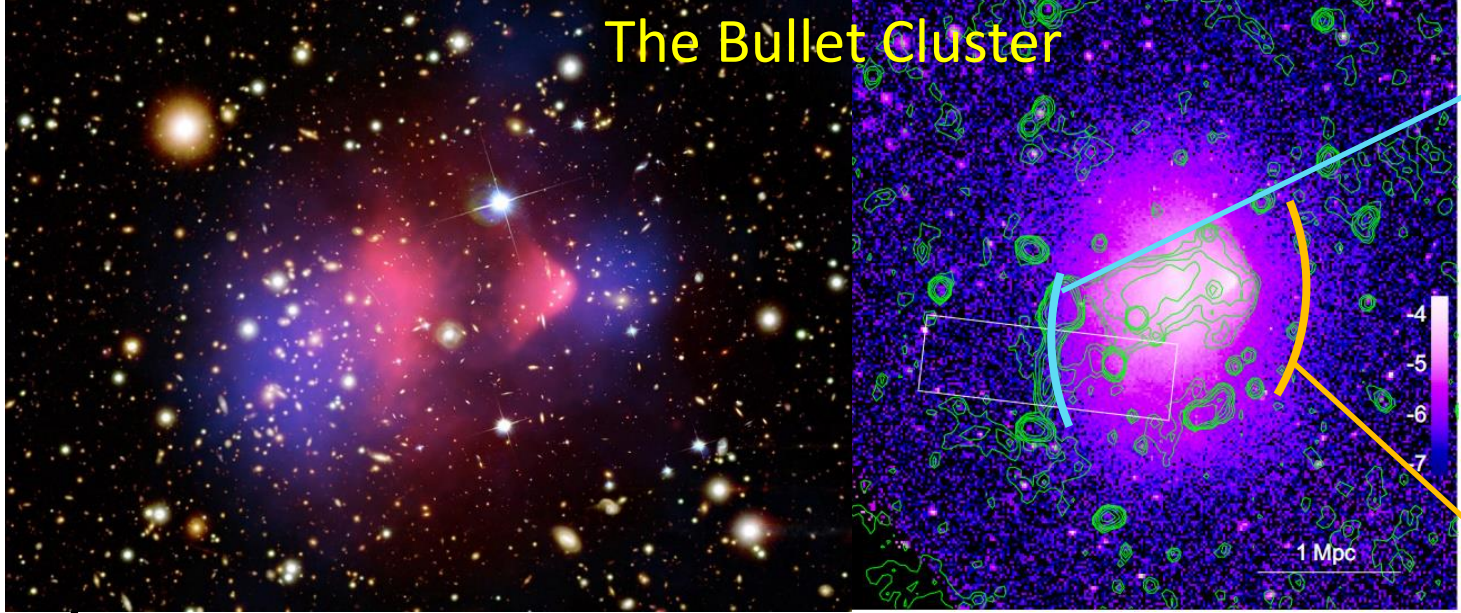
$$\rightarrow E_{\text{kinetic}} \sim 1/10 E_{\text{thermal}}, \quad E_{\text{magnetic}} \sim 1/10 E_{\text{kinetic}}, \quad \beta \sim 100$$

ICMs are highly dynamical

- large-scale flow motions
- shock waves
- cosmic-rays
- turbulent flow motions
- magnetic fields



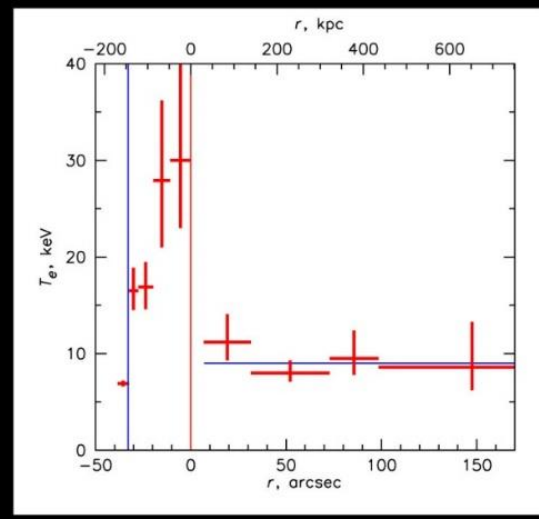
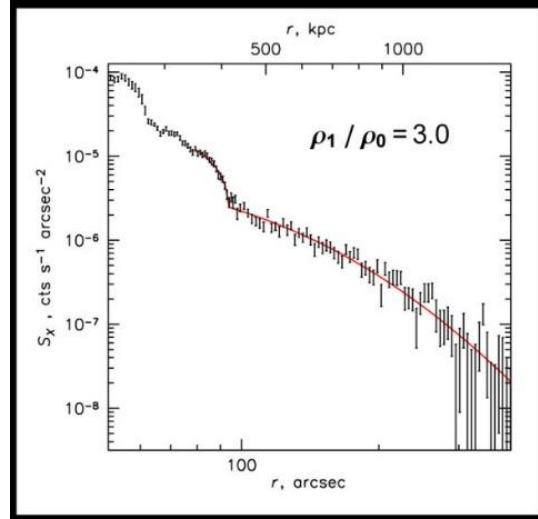
Observation of shocks in clusters: X-ray



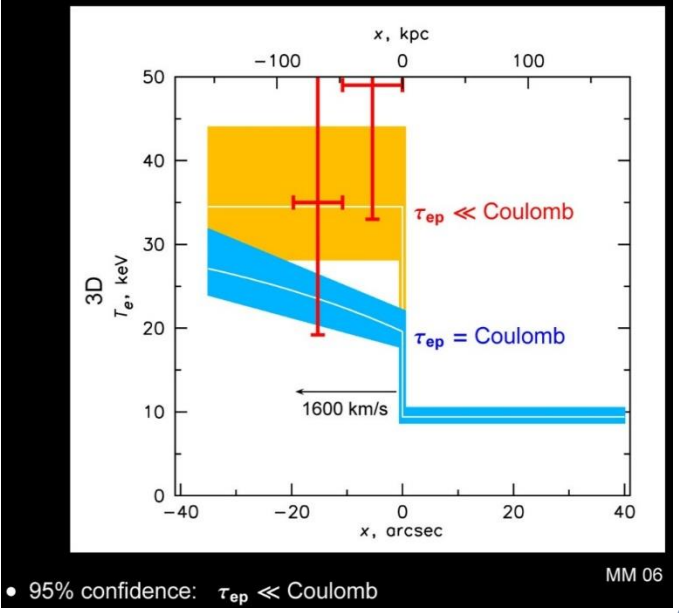
$M_X \approx 2.5$
Shimwell et al. 2015

$M_X \approx 3.0$
(no associated radio relic)
Markevitch 2006

Shock wave in
1E0657-56
(Bullet cluster)



$M = 3.0 \pm 0.4$, shock $v = 4700$ km/s

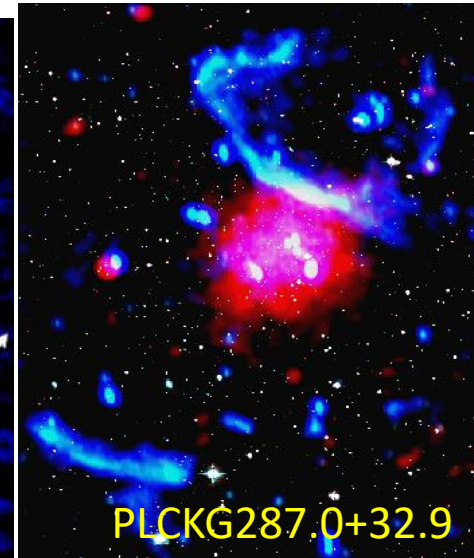
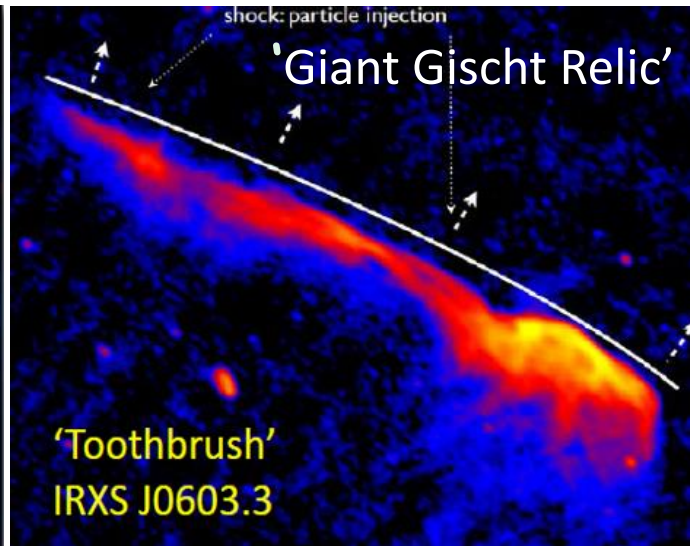
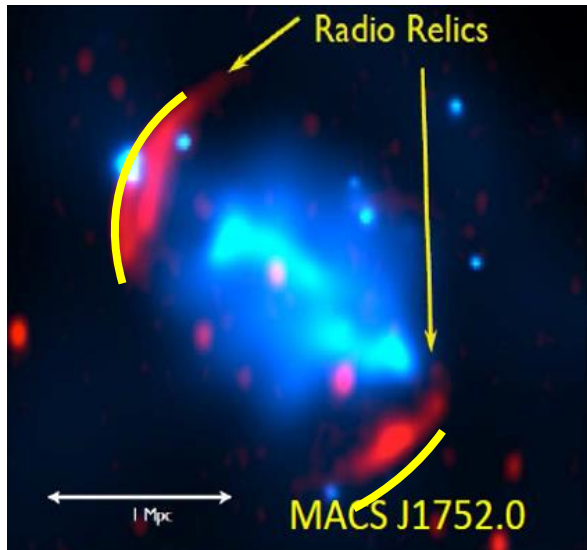


• 95% confidence: $\tau_{ep} \ll \text{Coulomb}$

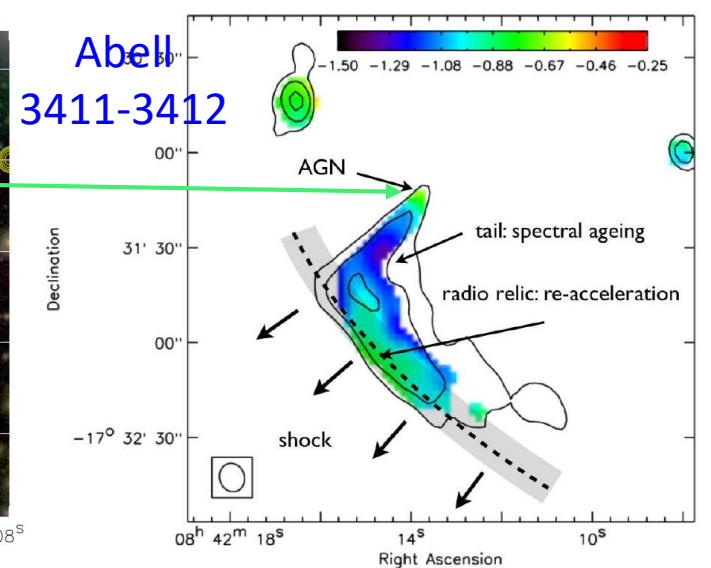
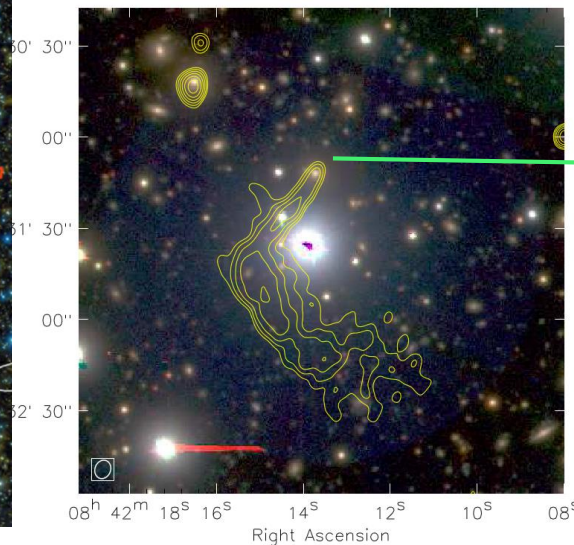
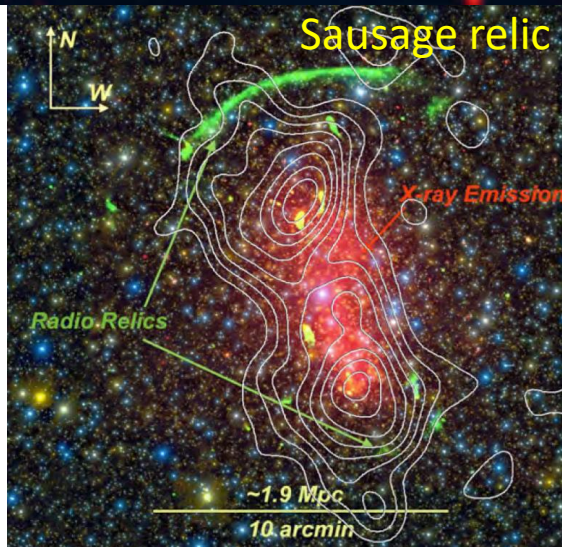
MM 06

Mach number of X-ray shocks in ICMs:
 $M_{\text{shock}} < \sim \text{a few}$

Observation of shocks in clusters: radio relics



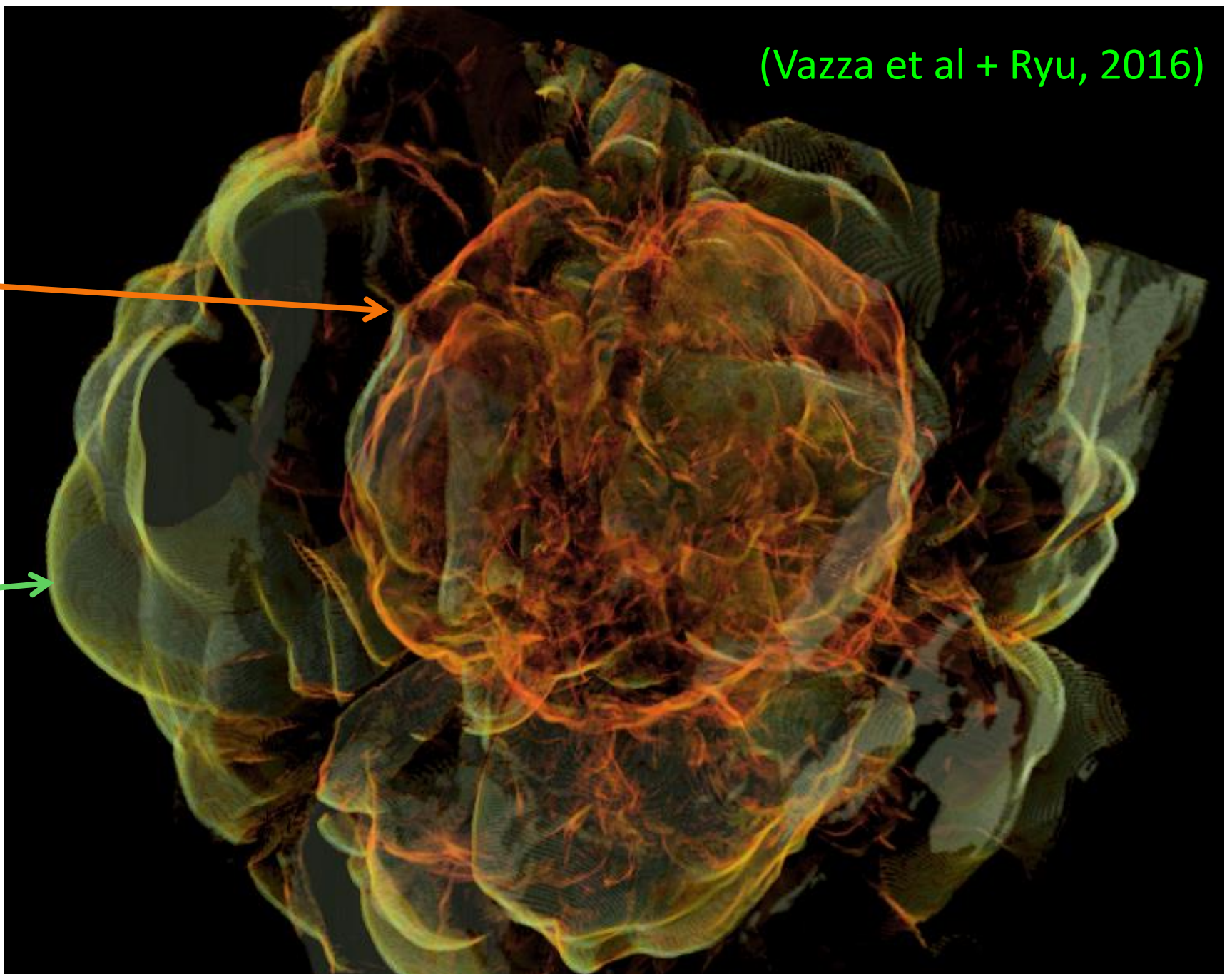
Mach number of
radio shocks in ICMs:
 $M_{\text{shock}} < \sim \text{several}$

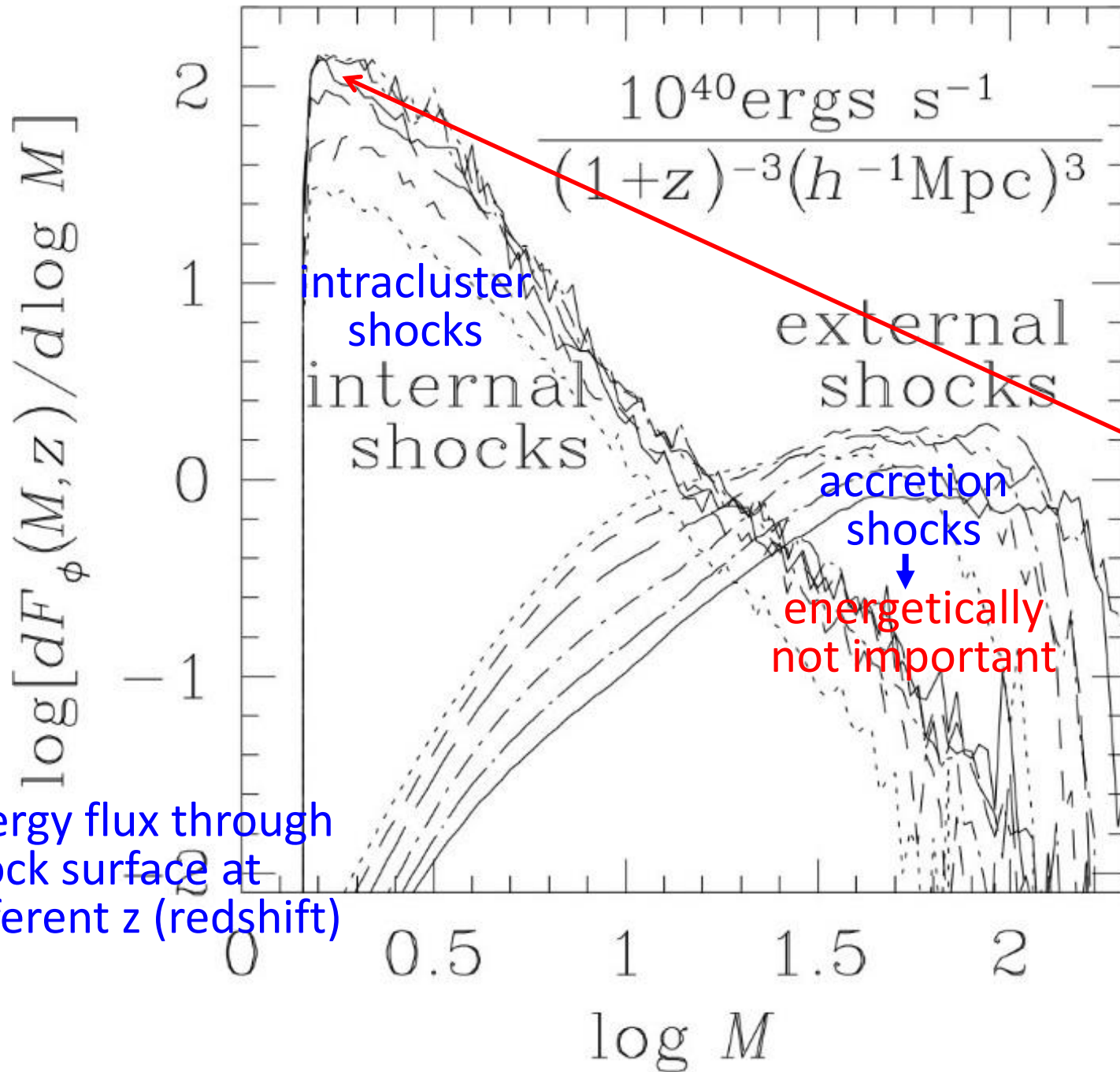


(Vazza et al + Ryu, 2016)

weak inreaccluster
shocks with $M < \text{a few}$
(orange)

strong accretion
shocks with $M > \sim 10$
(green)





Shock waves inside and around clusters

(Ryu et al. 2003)

Weak intracluster shocks with $M_s \sim$ a few, $V_s \sim 2,000$ km/s are energetically more important.

energy flux through shock surface at different z (redshift)

The nature of shock waves in clusters of galaxies during the hierarchical structure formation

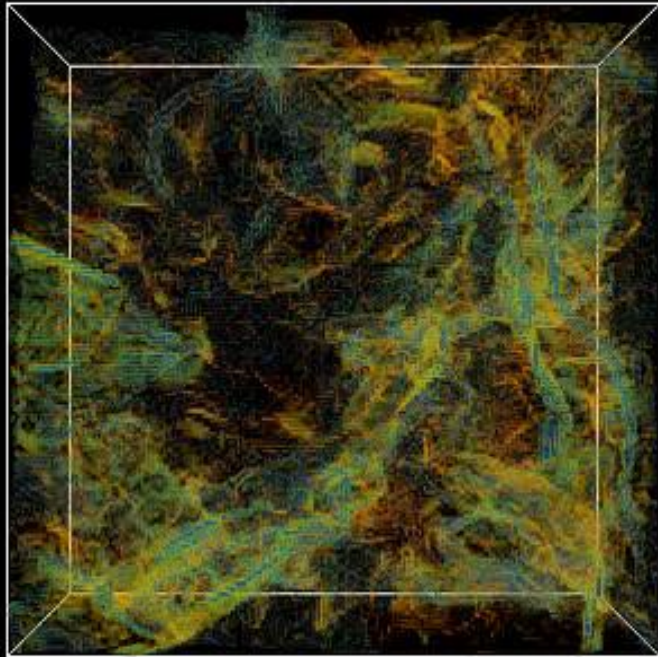
- 1) accretion shocks around clusters formed by accreting void gas
- 2) intracluster shocks inside cluster
 - a) turbulence shocks - induced by turbulent flow motions
 - b) infall shocks - accretion of the WHIM (Warm-Hot Intergalactic Medium) to the hot intracluster medium along filaments
 - c) merger shocks - induced by merger of gas/DM clumps during the hierarchical formation of galaxy clusters, $M_{\text{shock}} < \sim$ a few to several a major merger of $\sim 10^{13} - 10^{14} M_{\odot}$ of gas clumps with speed of $\sim 1,000$ km/s $\rightarrow E_{\text{merger}} \sim 10^{63} - 10^{64}$ ergs \rightarrow “energetically important”

Shock waves in a merging cluster from a simulation

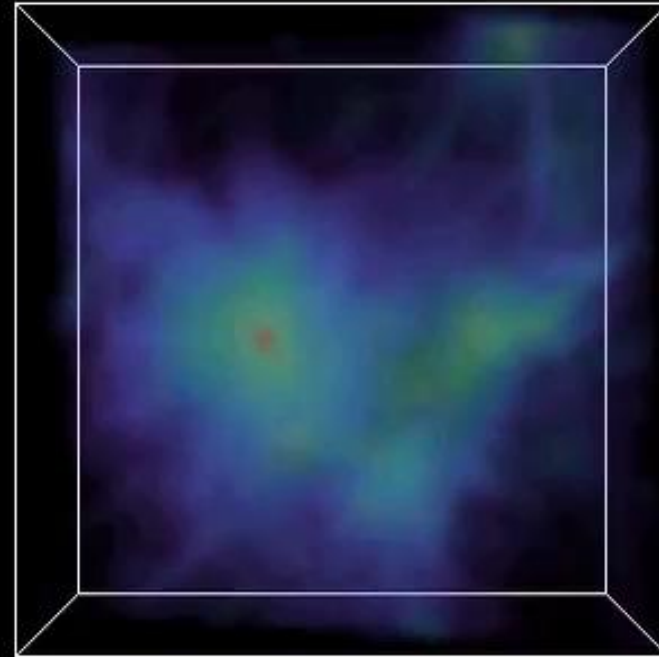
(Ha, Ryu, & Kang 2017)

from $z = 0.5$ to 0.05 , box size = $5 h^{-1}$ Mpc

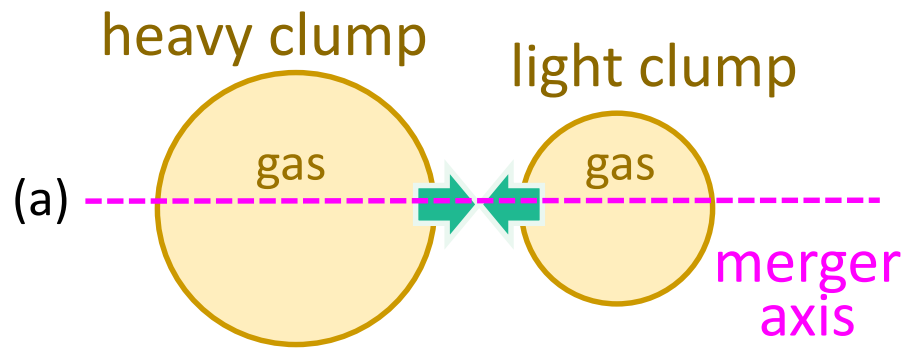
shocks with $1 < M_s < 10$



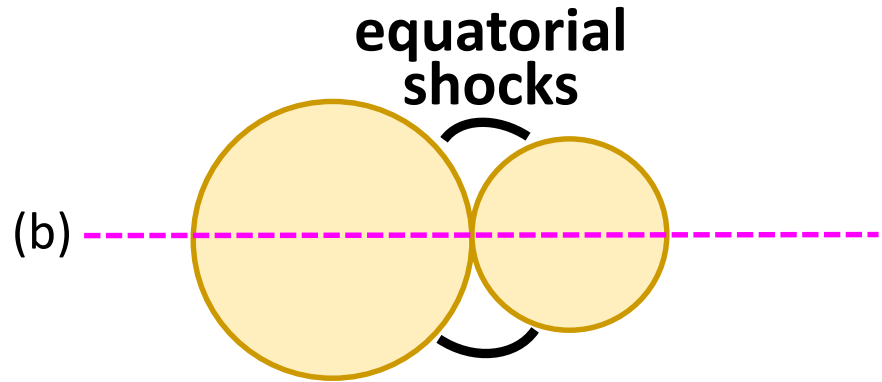
X-ray emissivity



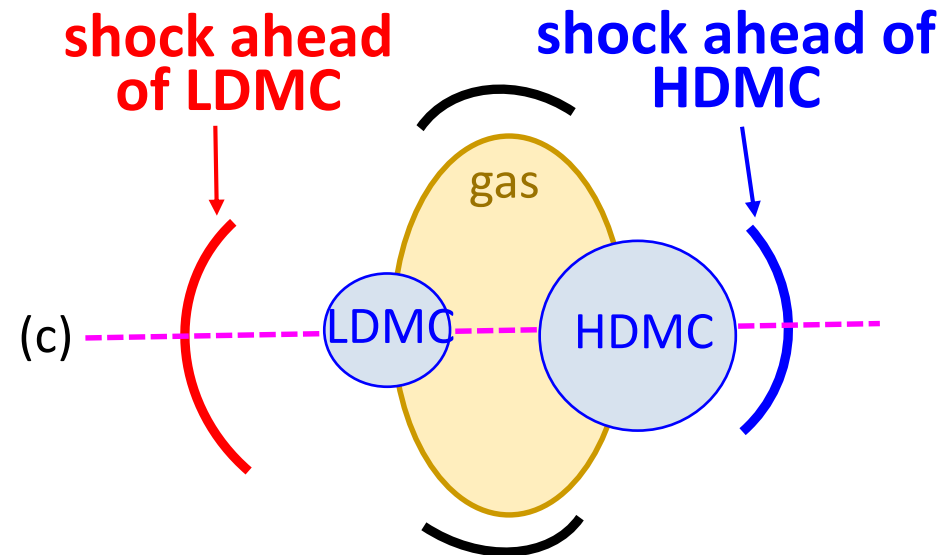
Simple binary merger – a cartoon picture



Two clumps are approaching.



Shocks along the direction perpendicular to the merger axis are first launched.

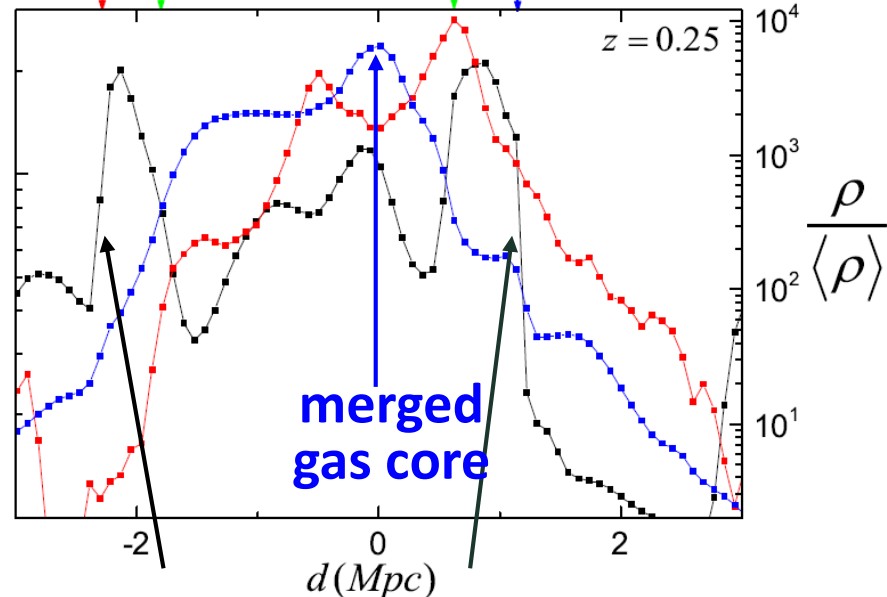
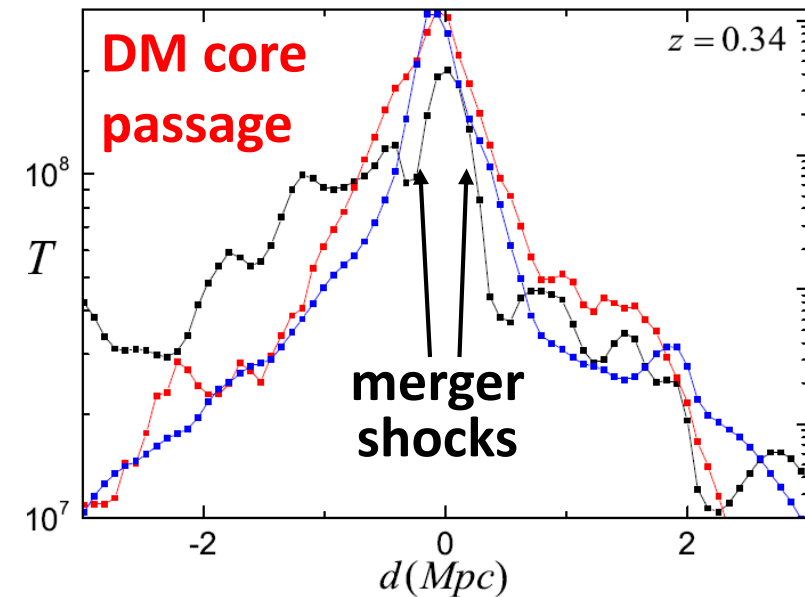
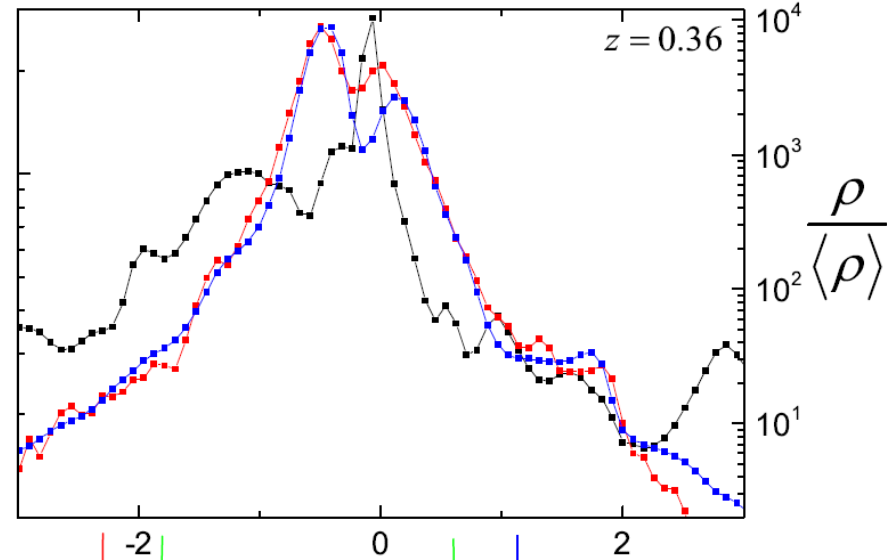
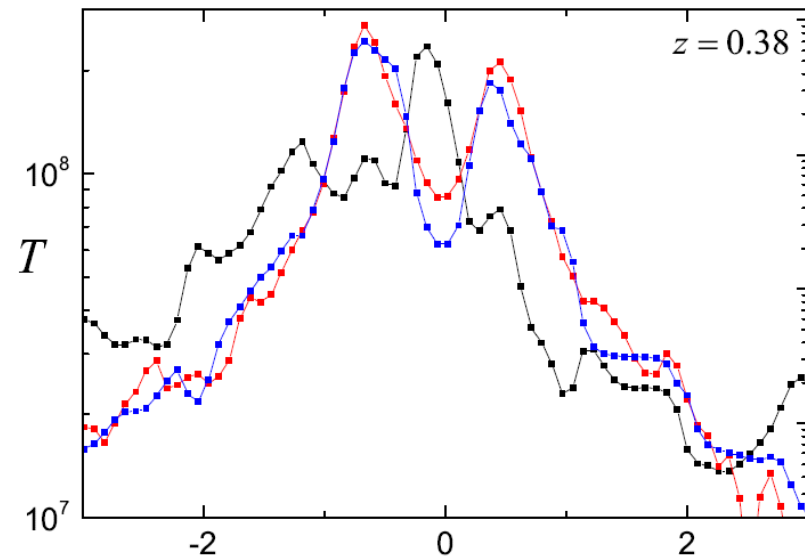


LDMC – light dark matter core

HDMC – heavy dark matter core

Shocks along the direction parallel to the merger axis form and propagate.

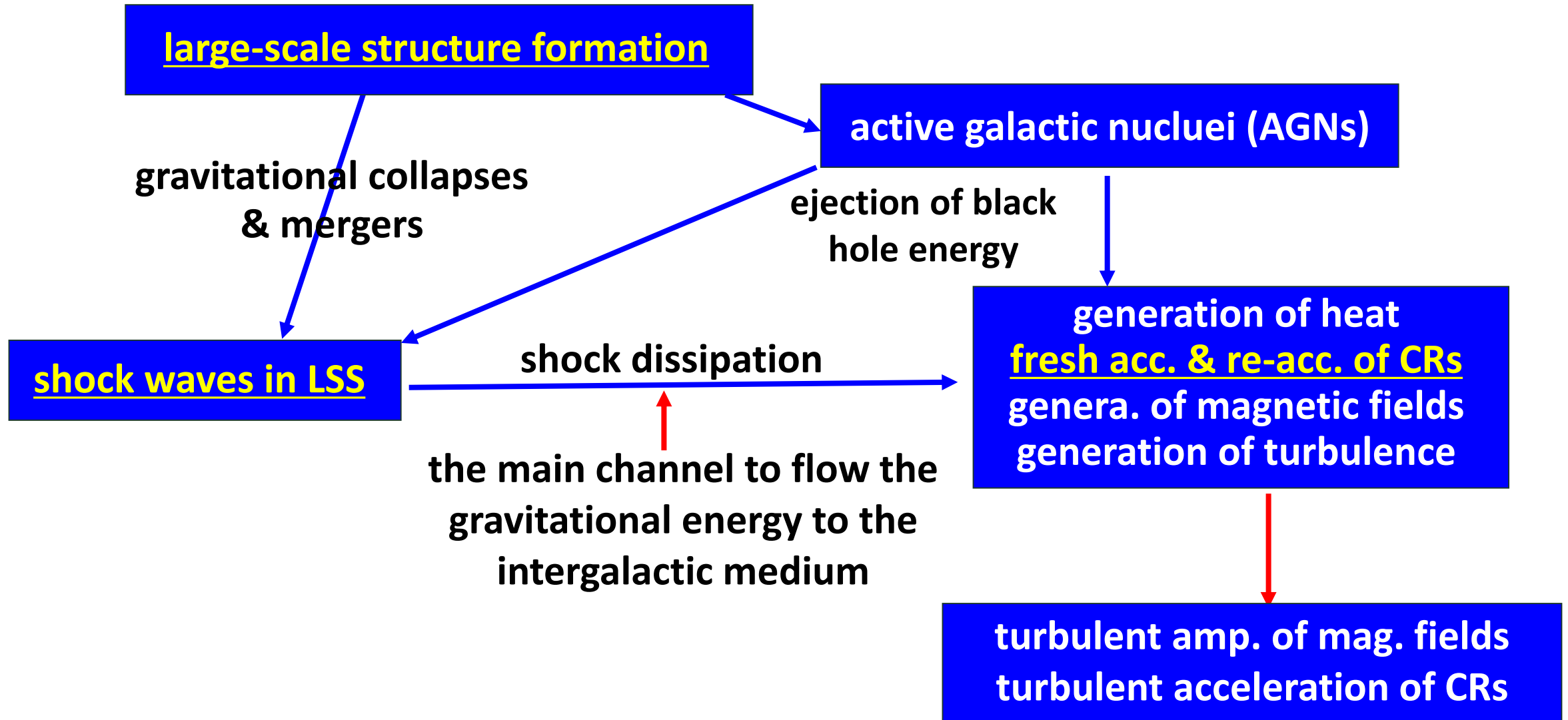
1D profiles along the merger axis at four epochs



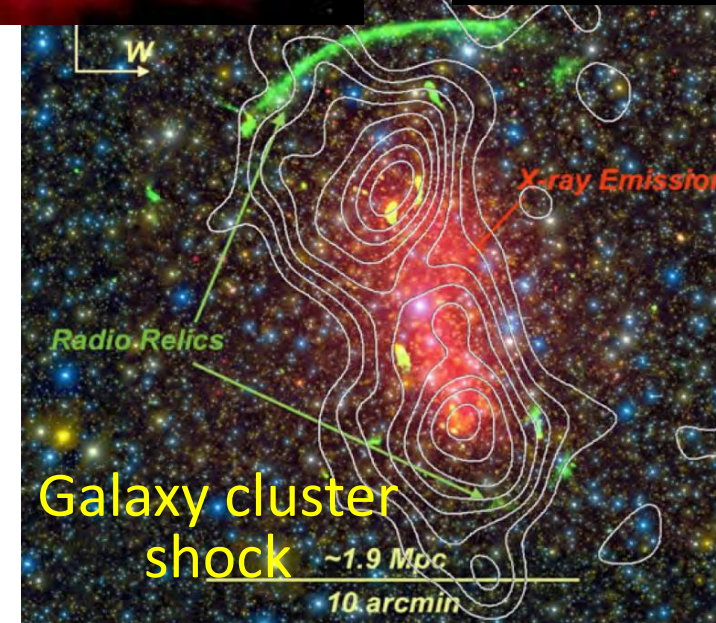
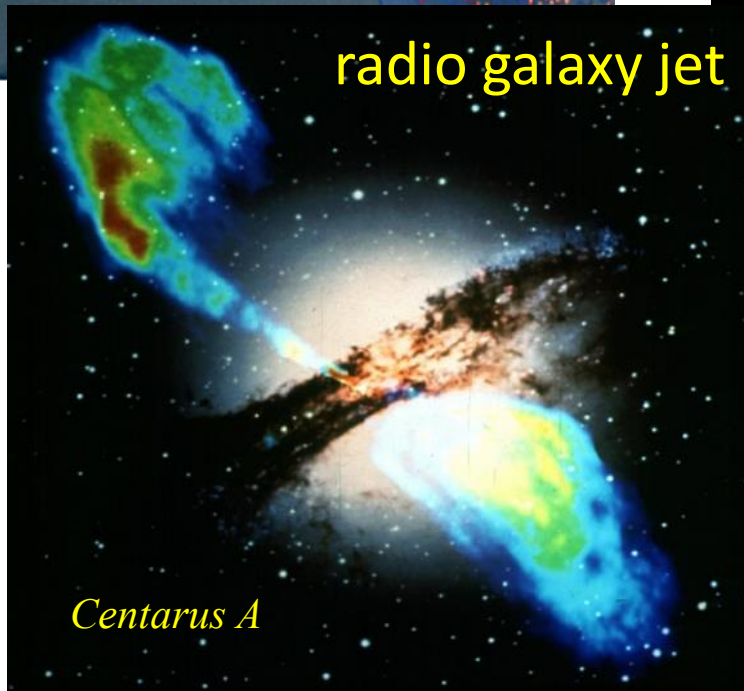
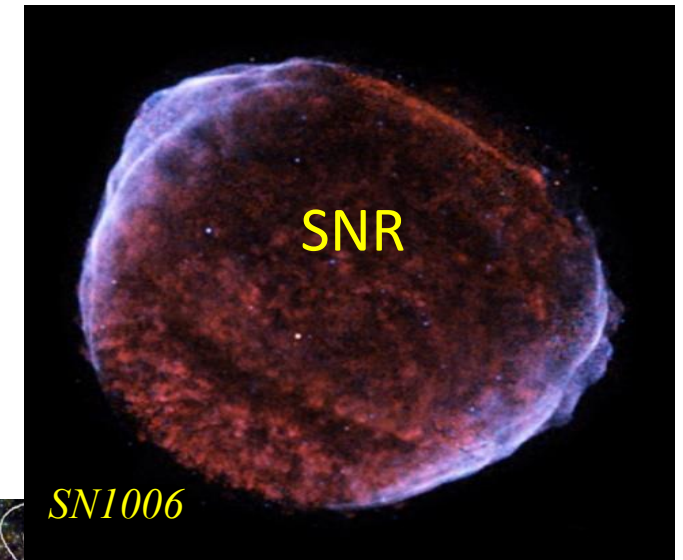
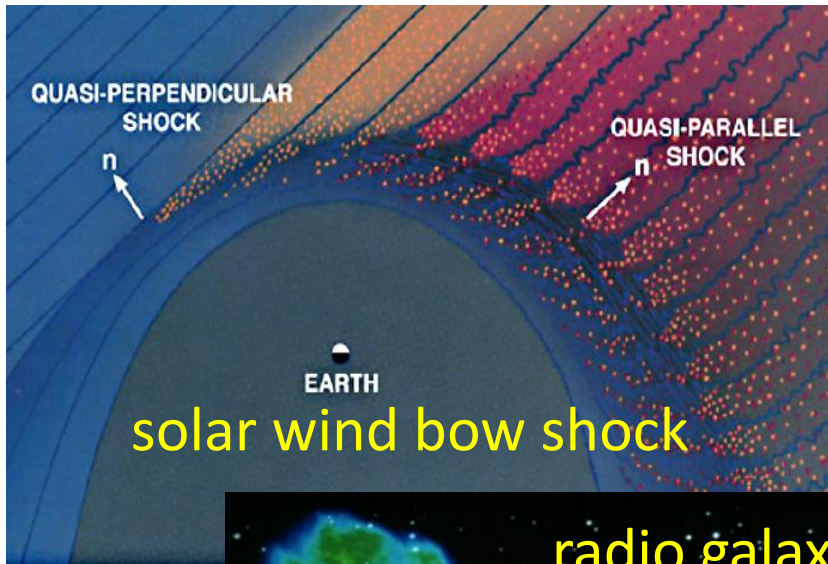
temperature
gas density
DM density

merger shocks of $M_s \sim 3$

Overview for the formation and roles of shock waves in the large-scale structure of the universe

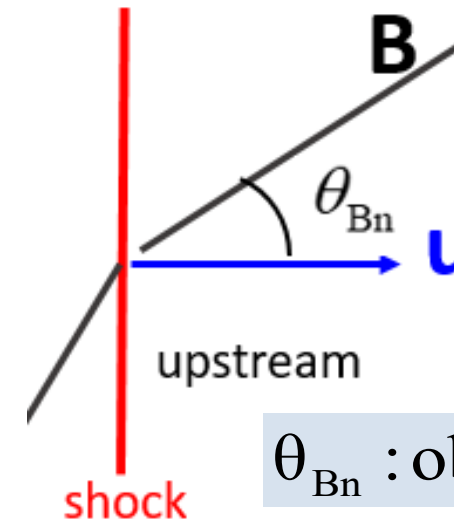


Shocks in astrophysical environments are collisionless, and CRs are accelerated at collisionless shocks !



Properties of astrophysical shocks

	solar wind (IPM)	interstellar medium (ISM)	intracluster medium (ICM)
size	$\sim 10^{12}$ cm	$\sim 10^{21}$ cm	$\sim 10^{25}$ cm
particle density	~ 10 cm ⁻³	~ 0.1 cm ⁻³	$\sim 10^{-3}$ cm ⁻³
gas temperature	$\sim 10^5$ K	$\sim 10^4$ K	$\sim 10^8$ K
B strength	$\sim 10^{-4}$ G	$\sim 10^{-5}$ G	$\sim 10^{-6}$ G
c_s (km/s)	~ 50	~ 15	$\sim 1,000$
c_A (km/s)	~ 50	~ 15	~ 100
$\beta = p_g/p_B$	~ 1	~ 1	~ 100
v_{shock} (km/s)	~ 500	$\sim 3,000$	$\sim 3,000$
M_s	~ 10	~ 200	~ 3
M_A	~ 10	~ 200	~ 30



θ_{Bn} : obliquity angle

$$M_A \approx \beta_p^{1/2} M_s$$

particle acceleration at collisionless shocks depend on $M_s, M_A, \theta_{Bn}, \beta_p, \alpha_p$

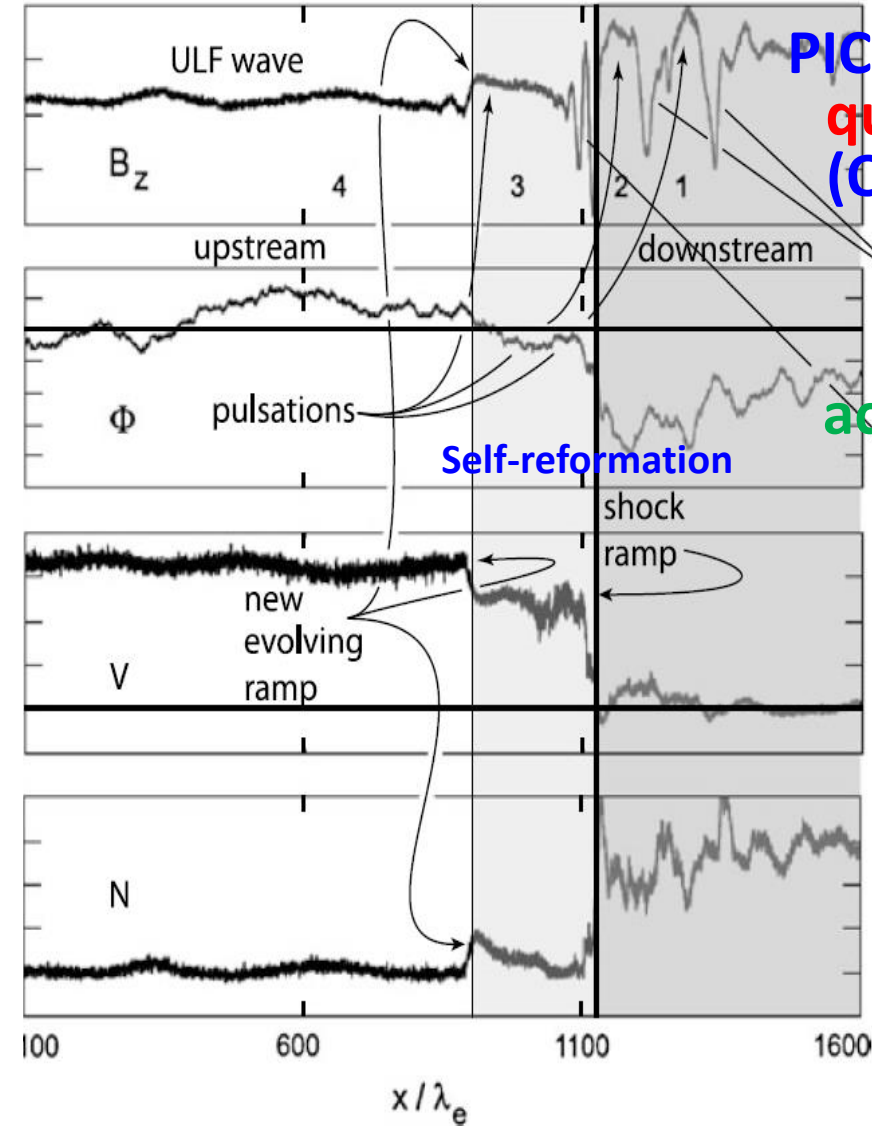
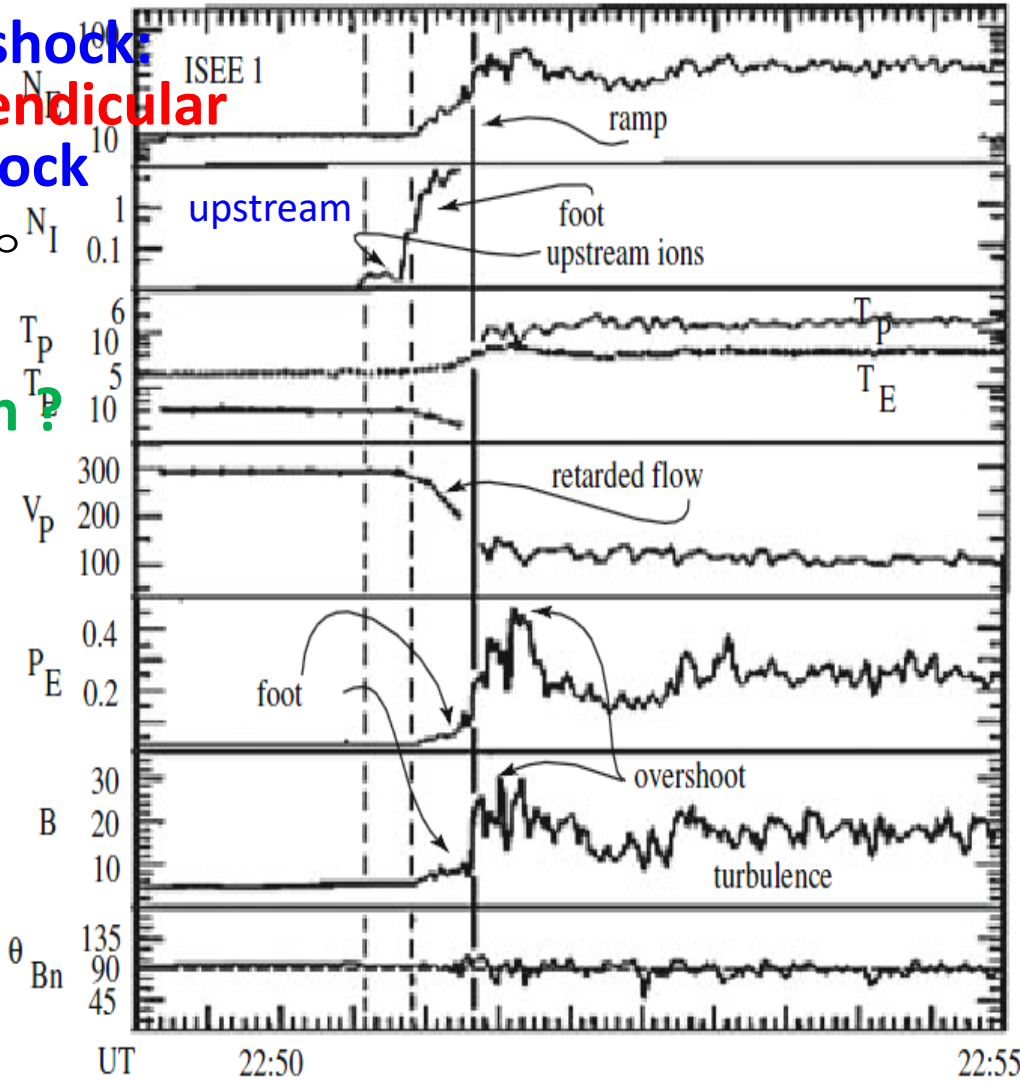
ICM shocks are fairly strong in terms of M_A , but weak in terms of M_s !

Collisionless shock is not a simple MHD jump

Earth Bow shock
quasi-perpendicular
(Q-perp) shock

$$\theta_{Bn} \geq 45^\circ$$

electron
acceleration ?



PIC simulation:
quasi-parallel
(Q-par) shock

$$\theta_{Bn} \leq 45^\circ$$

proton
acceleration ?

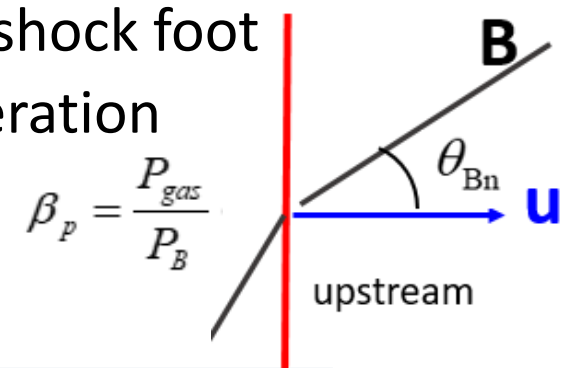
Dissipation is mediated by wave-particle interactions instead of inter-particle collisions.
→ complex kinetic processes, including microinstabilities, are involved.

Particle acceleration processes operating at collisionless shocks

- (1) Diffusive Shock Acceleration (DSA):** Fermi 1st order process
 - effective at **quasi-parallel (Q-par)** shocks $\theta_{Bn} \geq 45^\circ$
 - scattering off MHD waves in the upstream and downstream region
- (2) Shock Drift Acceleration (SDA)**
 - effective at **quasi-perpendicular (Q-perp)** shocks $\theta_{Bn} \leq 45^\circ$
 - drifting along the convective E field (grad B) at the shock front

← most important in ICM shocks

- (3) Shock Surfing Acceleration (SSA)**
 - effective at **quasi-perpendicular (Q-perp)** shocks
 - reflected by shock potential, scattered by upstream waves
 - moving along the convective E field, while being trapped at the shock foot
- (4) Turbulent Acceleration:** Fermi 2nd order process, stochastic acceleration
 - much less efficient than DSA
 - could be important only in turbulent plasma

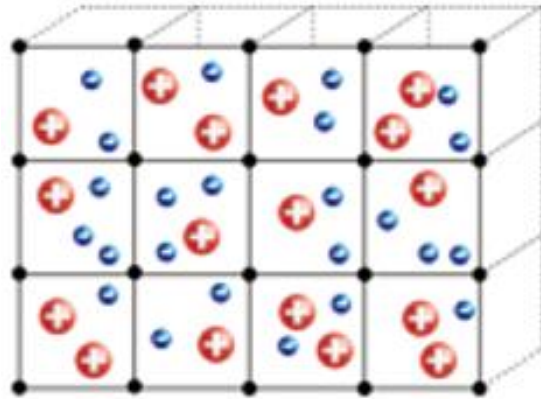


$$\beta_p = \frac{P_{gas}}{P_B}$$

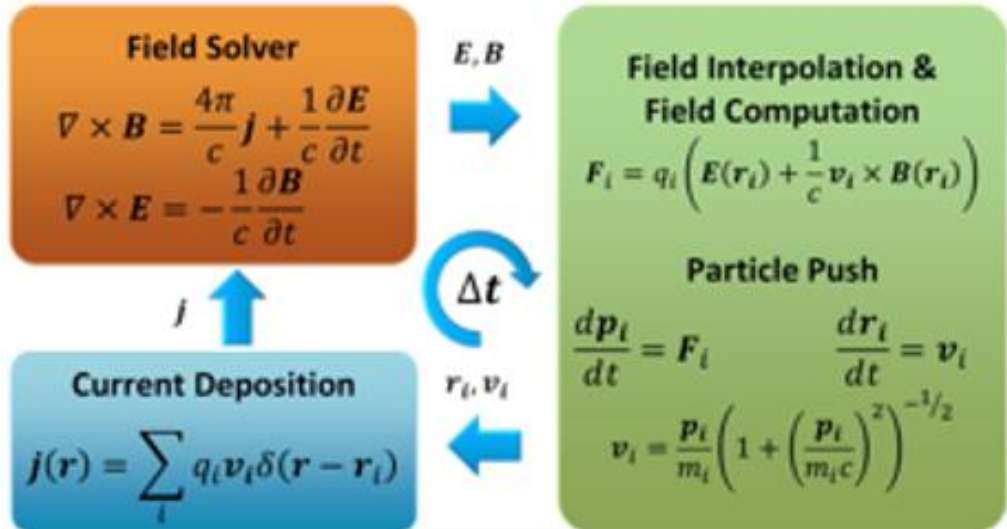
Previous studies on collisionless shocks focus mainly on low beta (<1) plasma (e.g. solar wind & ISM). Physics of **weak shocks in beta=100 ICM** (including various microinstabilities) could be quite different.

Simulations to study kinetic processes at collisionless shocks

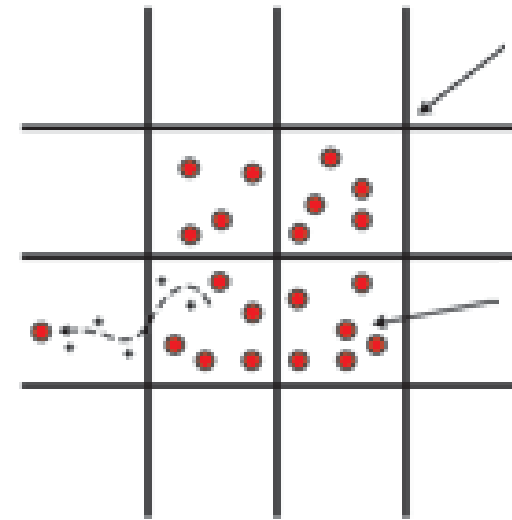
Particle-in-Cell (PIC) approach



proton particles +
electron particles



hybrid approach



electron

proton particles
+ electron fluid

proton

$$\omega_{pe}/\omega_{pi} = \sqrt{m_i/m_e} = 43$$

large mass ratio of p and e

→ large ratio of involved time scales

→ hybrid code runs much faster than PIC code

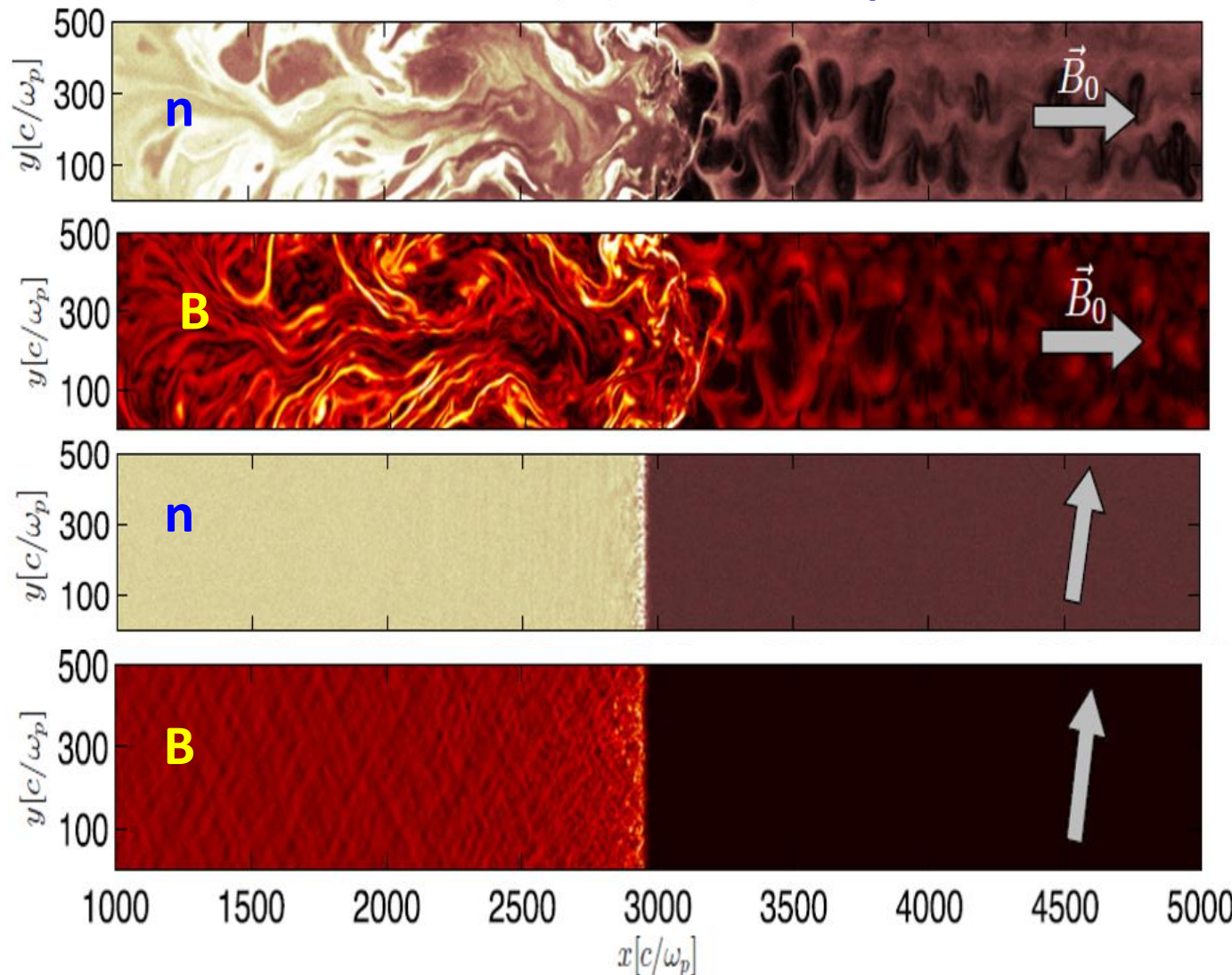
Hybrid simulation: proton acceleration at shocks

$$\beta = \beta_e + \beta_p \approx 1, M_A \sim M_s = 20 \quad M_A \approx \beta_p^{1/2} M_s$$

(Caprioli & Spitkovsky 2014)

downstream

upstream



At parallel shocks

Stream of accelerated ions into upstream

→ self-generated waves

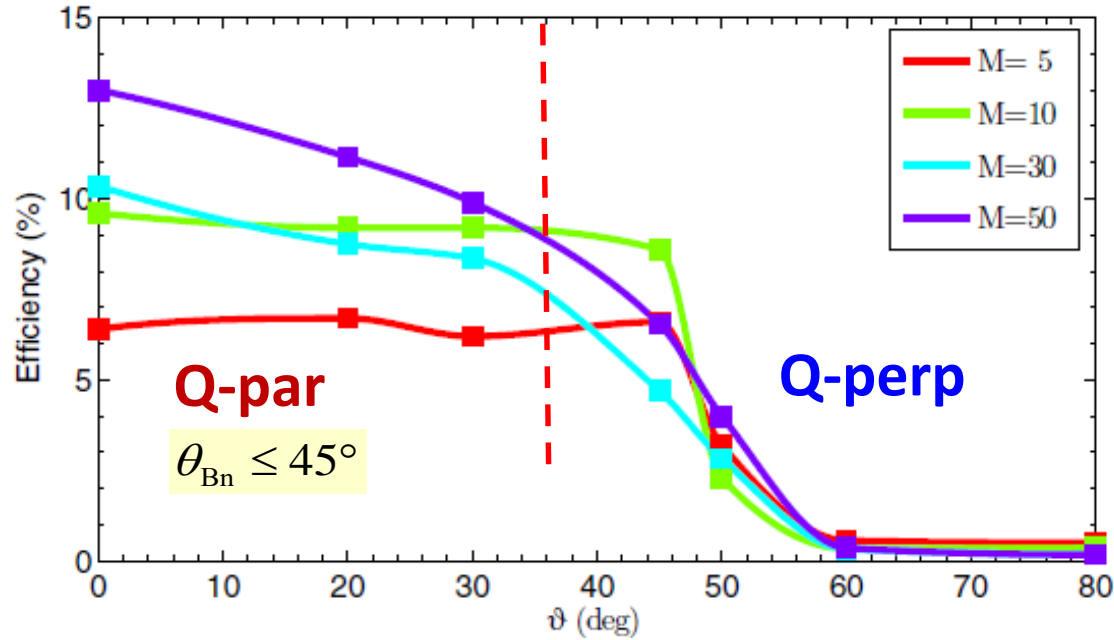
→ B amplification & efficient CR acceleration

At Q-perp shocks

No backstreaming ions into upstream

→ No turbulent waves are excited

CR proton acceleration efficiency from hybrid simulations



$$\eta \equiv \frac{E_{CR} u_2}{1/2 \rho V_s^3} \quad \beta_p = \frac{P_{gas}}{P_B} \approx 1$$

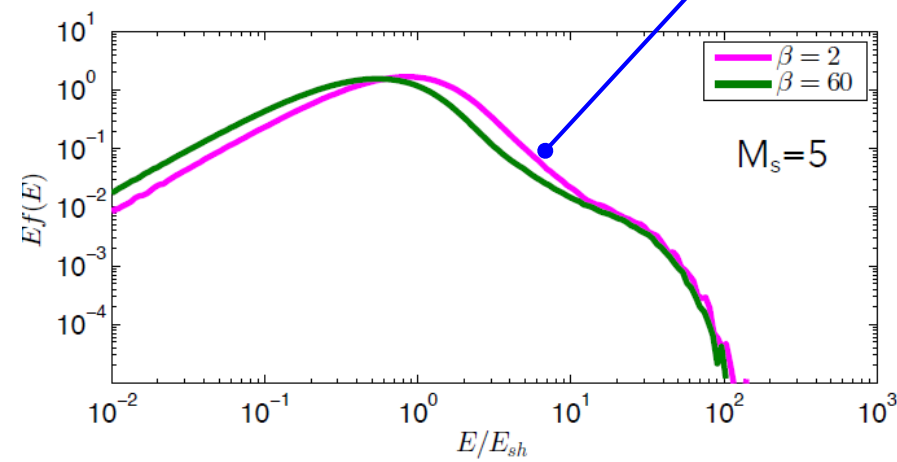
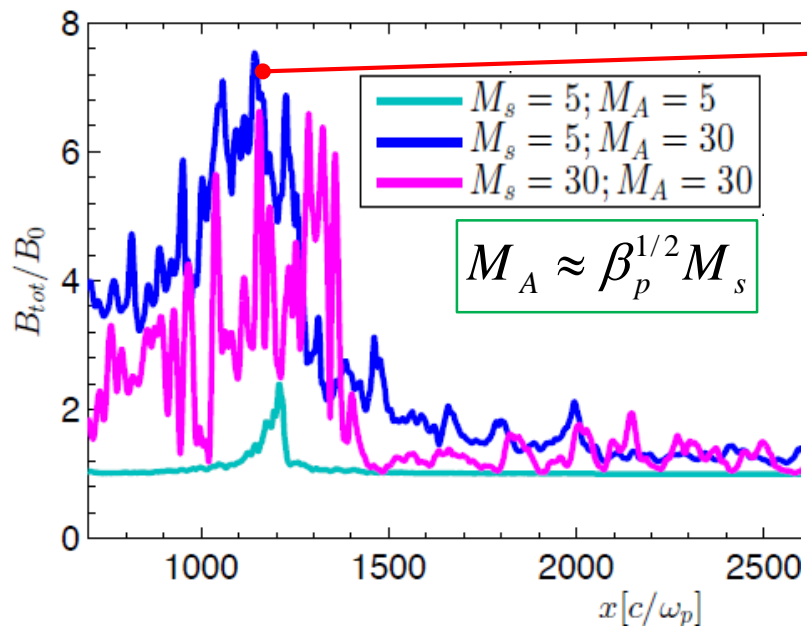
$\eta \approx 0.05$ for $M_s = 5$

at quasi-parallel shocks

– $\eta \sim M_s$ (%) for $M_s < 5$

– B amplification is controlled by M_A

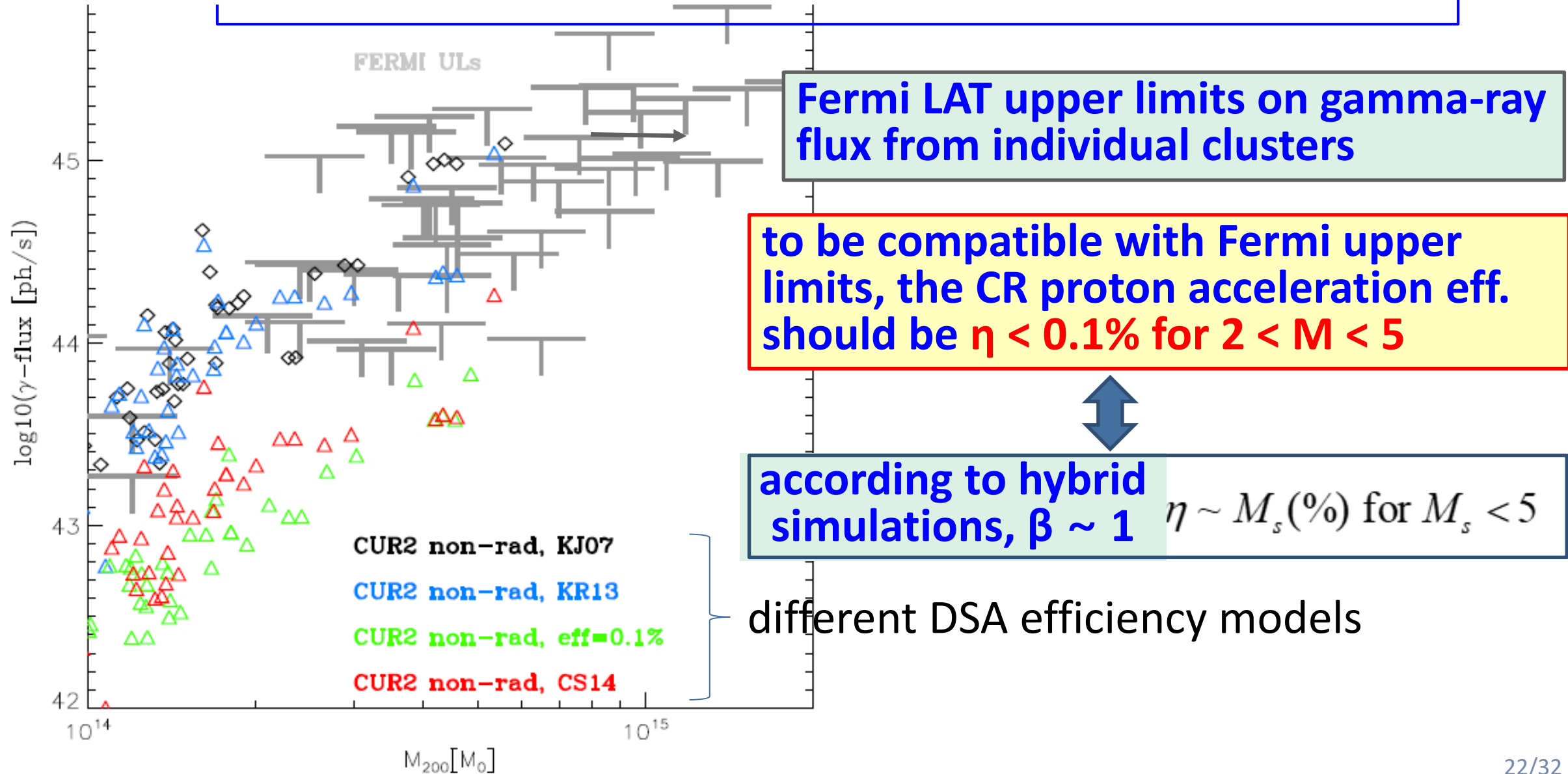
– CR acceleration is governed by M_s



High beta cases
(Caprioli 2017 KAW9)

Constraining the efficiency of cosmic ray acceleration by cluster shocks

F. Vazza,¹★ M. Brüggen,¹ D. Wittor,¹ C. Gheller,² D. Eckert³ and M. Stubbe¹ 2016

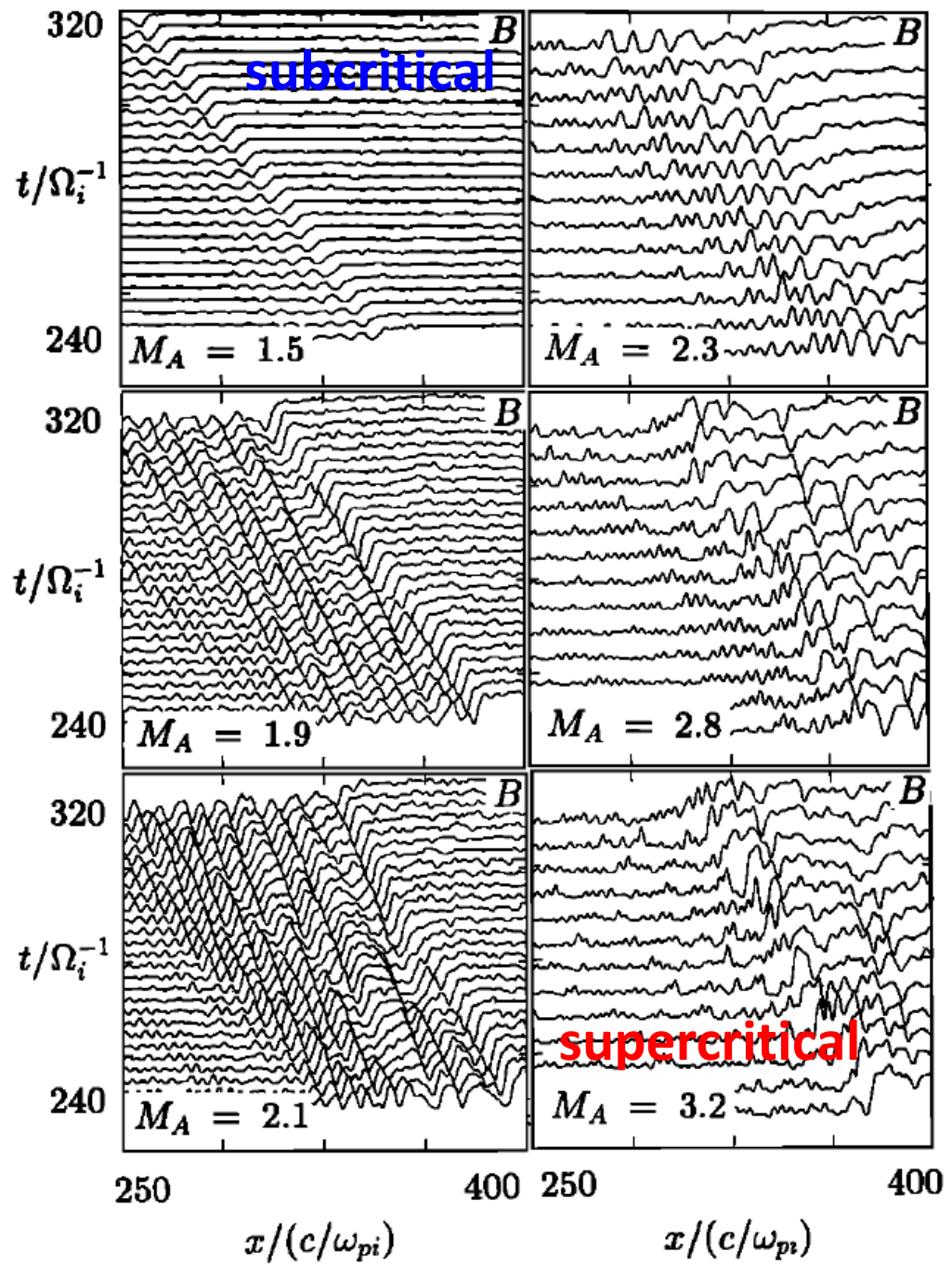


Low M_A Q-par shocks in sim.

1D hybrid simulations $\theta_{Bn} = 30^\circ$, $\beta_i = 0.5$

$M_A = 1.5$ the shock is steady & smooth.

For higher M_A , the shock is unsteady and supercritical and undergoes self-reform.



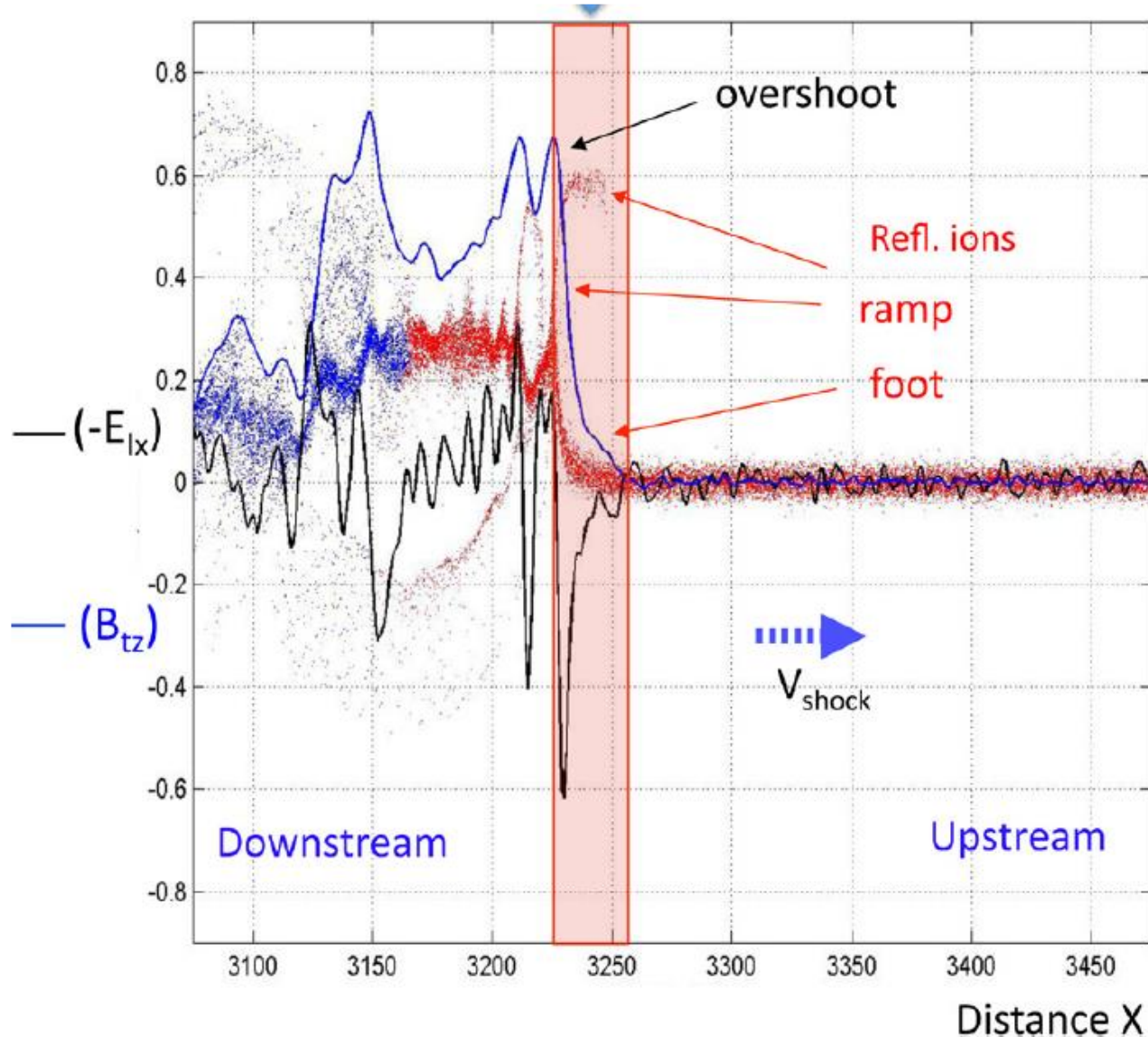
subcritical weak shocks

- shock transition is smooth, lacking an overshoot
- no reflected ions, no particle acceleration

SOURCES OF MAGNETOSHEATH WAVES AND TURBULENCE

N. Omidi,* A. O'Farrell** and D. Krauss-Varban*** 1994

Structure of supercritical perpendicular shock



If $M > M_{\text{crit}}$ (supercritical),
a large fraction of incoming ions
are reflected back to upstream.

$\beta = 0$ limit (Edmiston & Kennel 1984)

$$M_f^* = 1.53 \text{ for } \theta_{Bn} = 0^\circ$$

$$M_f^* = 2.76 \text{ for } \theta_{Bn} = 90^\circ$$

- relative drift between reflected ions and incoming particles excites various micro-instabilities in the shock foot.

→ shock criticality is crucial for particle acceleration

1D & 2D PIC simulations for Q-par shocks (proton acceleration) using TRISTAN-MP

(Ha, Ryu, Kang, van Marle 2018)

Table 1. Model Parameters for the Simulations

Model Name	$M_s \approx M_f$	M_A	v_0/c	θ_{Bn}	β	$T_e = T_i$ [K(keV)]	m_i/m_e
M3.2 ^b	3.2	29.2	0.052	13°	100	$10^8(8.6)$	100
M2.0	2.0	18.2	0.027	13°	100	$10^8(8.6)$	100
M2.15	2.15	19.6	0.0297	13°	100	$10^8(8.6)$	100
M2.25	2.25	20.5	0.0315	13°	100	$10^8(8.6)$	100
M2.5	2.5	22.9	0.035	13°	100	$10^8(8.6)$	100
M2.85	2.85	26.0	0.0395	13°	100	$10^8(8.6)$	100
M3.5	3.5	31.9	0.057	13°	100	$10^8(8.6)$	100
M4	4.0	36.5	0.066	13°	100	$10^8(8.6)$	100
M3.2- θ 23	3.2	29.2	0.052	23°	100	$10^8(8.6)$	100
M3.2- θ 33	3.2	29.2	0.052	33°	100	$10^8(8.6)$	100
M3.2- θ 63	3.2	29.2	0.052	63°	100	$10^8(8.6)$	100
M2.0- β 30	2.0	10.0	0.027	13°	30	$10^8(8.6)$	100
M2.0- β 50	2.0	12.9	0.027	13°	50	$10^8(8.6)$	100
M3.2- β 30	3.2	16.0	0.052	13°	30	$10^8(8.6)$	100
M3.2- β 50	3.2	20.6	0.052	13°	50	$10^8(8.6)$	100
M2.0-m400	2.0	18.2	0.013	13°	100	$10^8(8.6)$	400
M2.0-m800	2.0	18.2	0.009	13°	100	$10^8(8.6)$	800
M3.2-m400	3.2	29.2	0.026	13°	100	$10^8(8.6)$	400
M3.2-m800	3.2	29.2	0.018	13°	100	$10^8(8.6)$	800

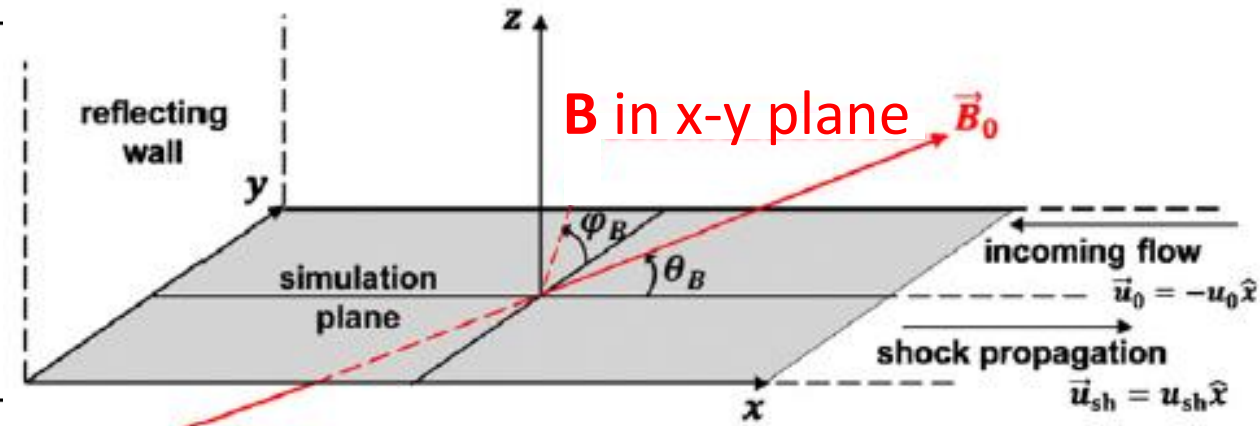


Figure 1. Simulation setup.

$$M_0 \equiv \frac{u_0}{c_s} = \frac{u_0}{\sqrt{2\Gamma k_B T_i / m_i}}$$

$$M_s \equiv \frac{u_{sh}}{c_s} \approx M_0 \frac{r}{r-1}$$

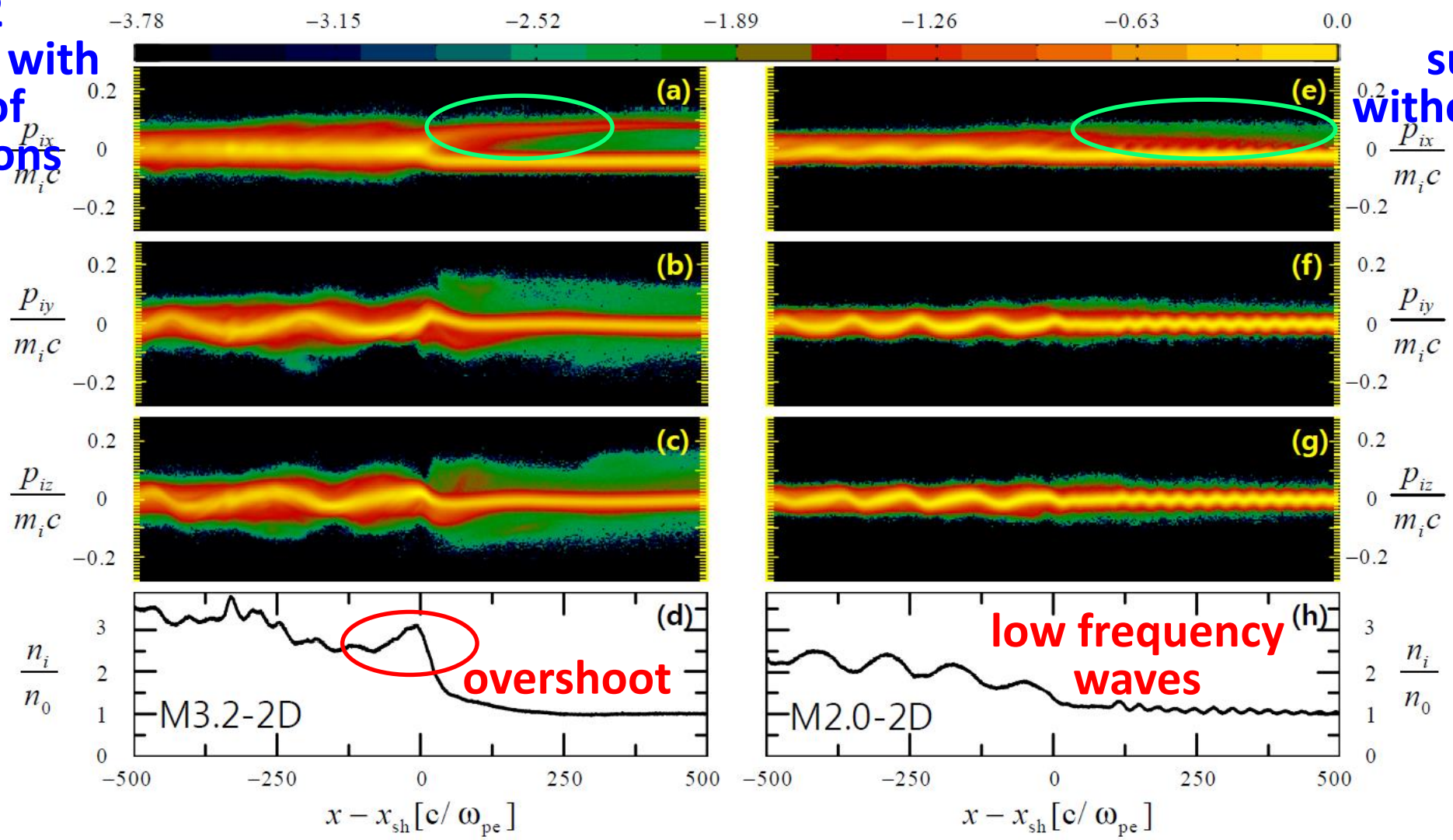
$$M_A \equiv \frac{u_{sh}}{v_A} \approx \sqrt{\beta} \cdot M_s$$

Structure of simulated Q-par shocks

$\theta_{Bn} = 13^\circ$

$M_s = 3.2$
supercritical with
a beam of
reflected ions

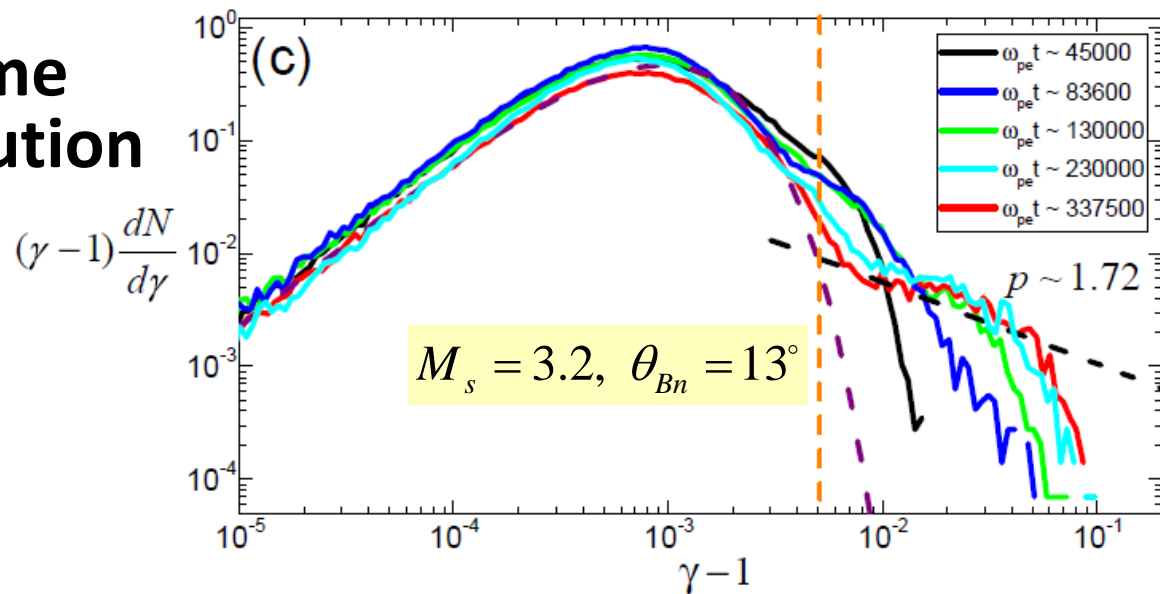
$M_s = 2.0$
subcritical
without reflected
ions



$$r_{L,i} \equiv \frac{m_i v_0 c}{e B_0} = M_{A,0} \sqrt{\frac{m_i}{m_e}} \frac{c}{w_{pe}} \sim 200 \frac{c}{w_{pe}}$$

Proton downstream energy spectrum of simulated shocks

time evolution

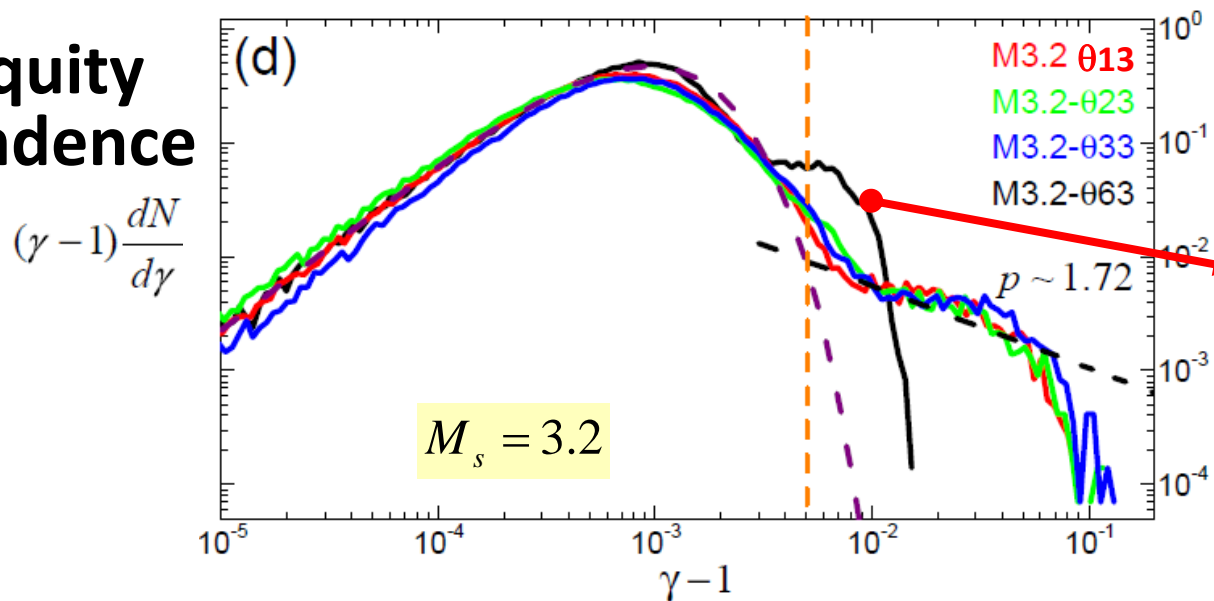


power-law spectrum extends to higher energy in time.

early stage of DSA in Q-par shocks

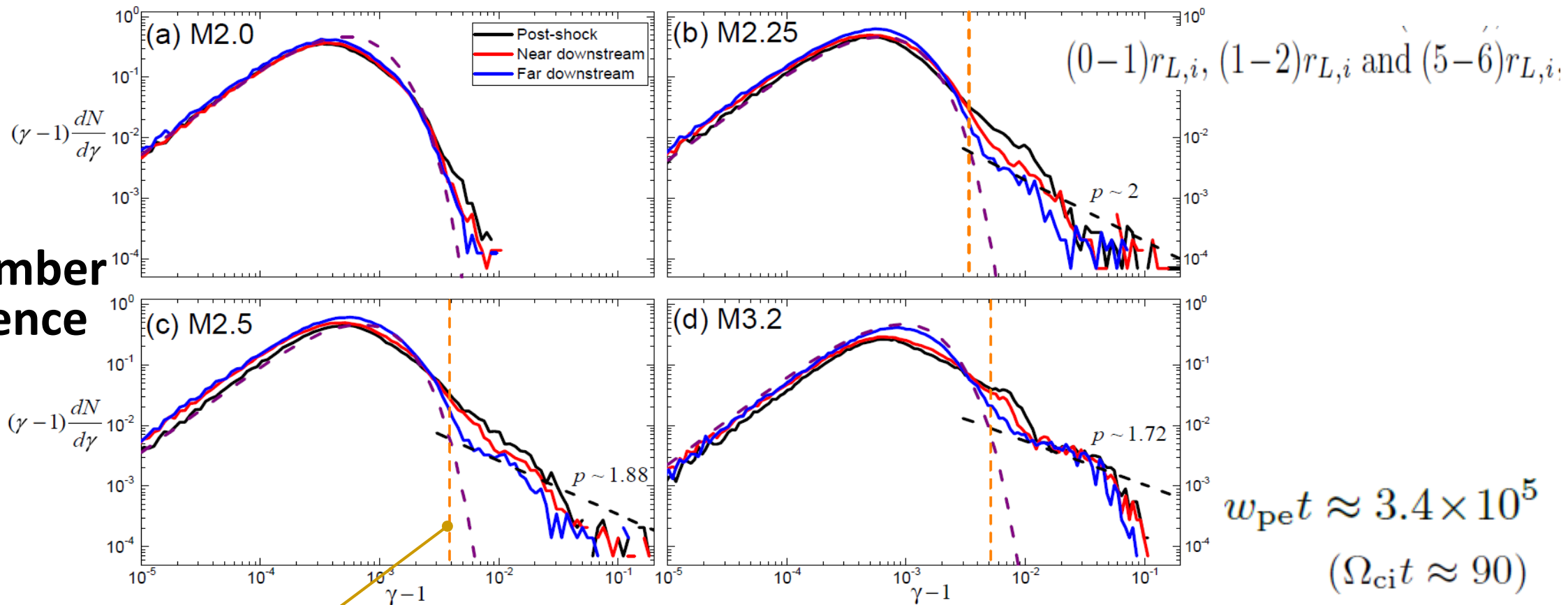
$$w_{pe} t \approx 3.4 \times 10^5 \quad (\Omega_{ci} t \approx 90)$$

obliquity dependence



only SDA (no DSA) in Q-perp shocks $\theta = 63$

Mach number dependence

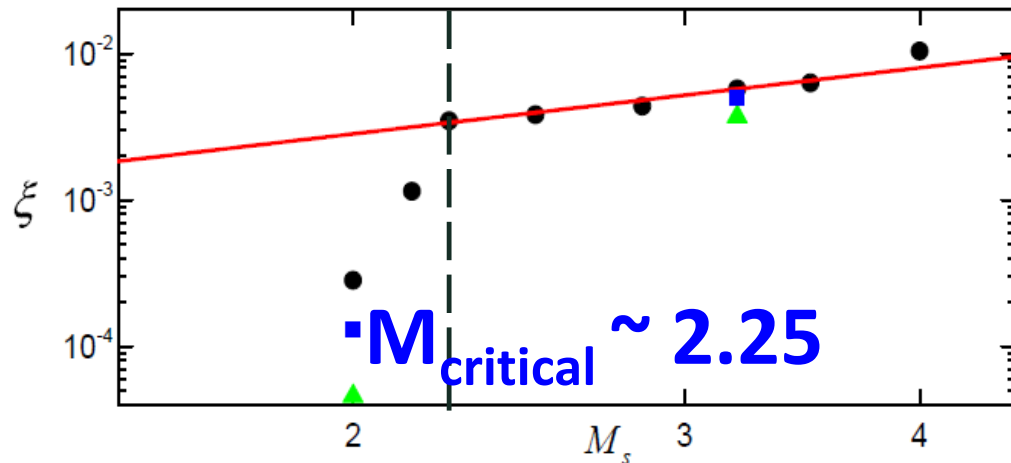


injection momentum

$$p_{\text{inj}} \approx 2.7 p_{\text{th}}, \text{ where } p_{\text{th}} = \sqrt{2m_i k_B T_2}$$

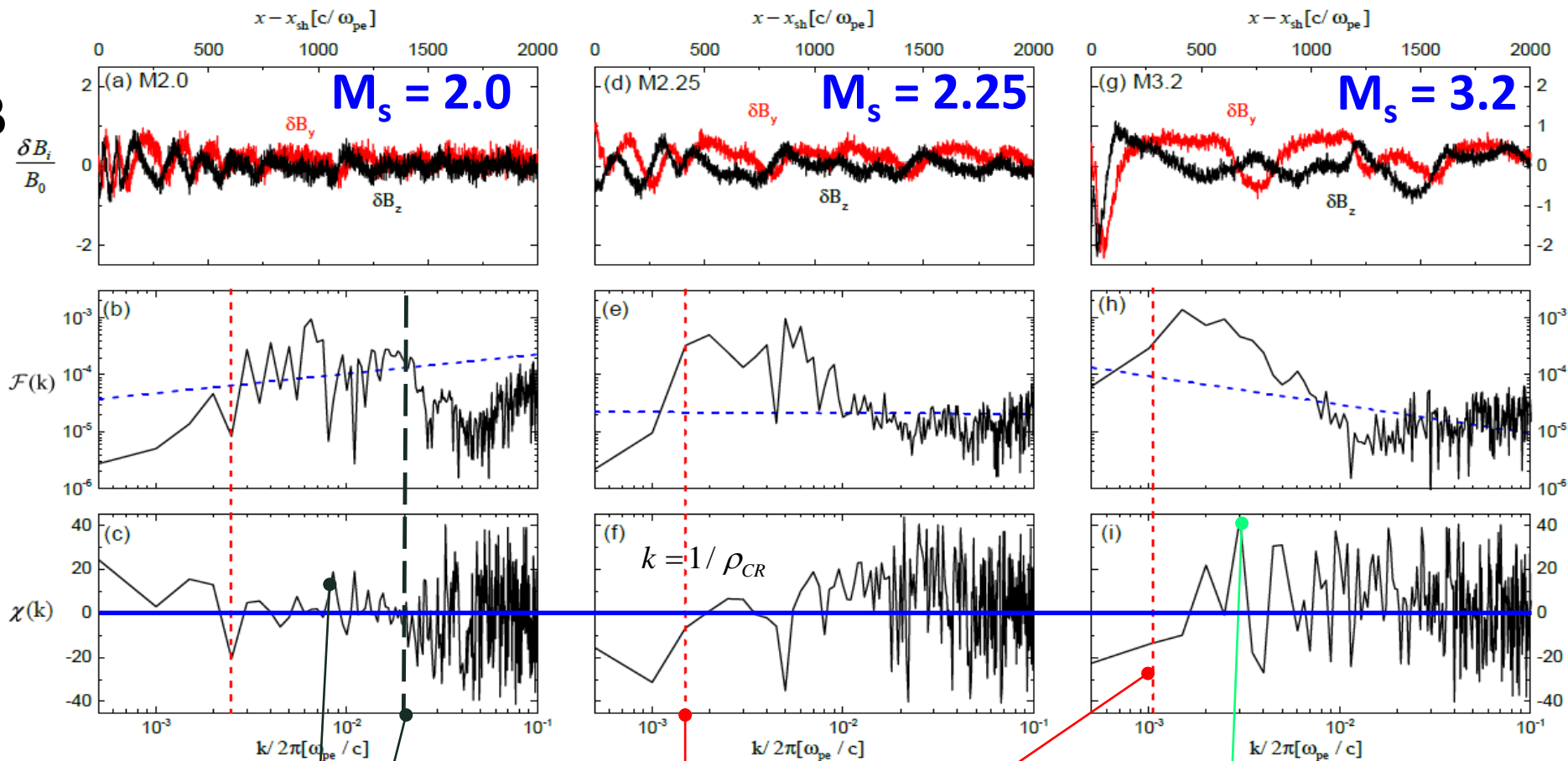
injection fraction

$$\xi \equiv \frac{1}{n_2} \int_{p_{\text{min}}}^{p_{\text{max}}} 4\pi f(p) p^2 dp, \quad p_{\text{min}} = \sqrt{2} p_{\text{inj}}$$



Waves in upstream of simulated shocks

Transverse components of B
 $\delta B / B \sim 1$



magnetosonic whistlers: $\frac{ck}{\omega_{pi}} \leq 1$

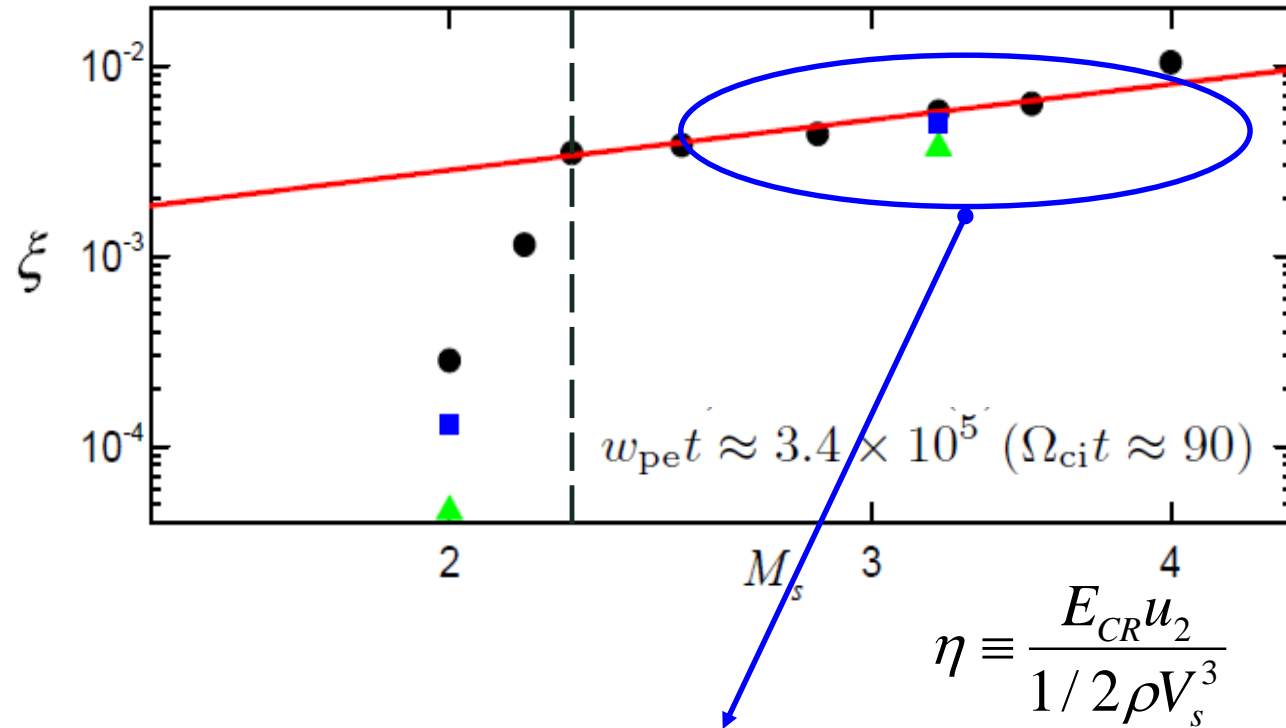
$$\frac{ck}{\omega_{pe}} \leq 0.1 \quad \text{with } m_i / m_e = 100$$

resonant mode (left-handed pol, $\chi = -45$)

non-resonant (right-handed pol, $\chi = +45$)

$$F(k) \propto k \left(\frac{\delta B}{B_0} \right)^2 \propto k^{q-5}, \quad f(p) \propto p^{-q}$$

Injection fraction and acceleration efficiency

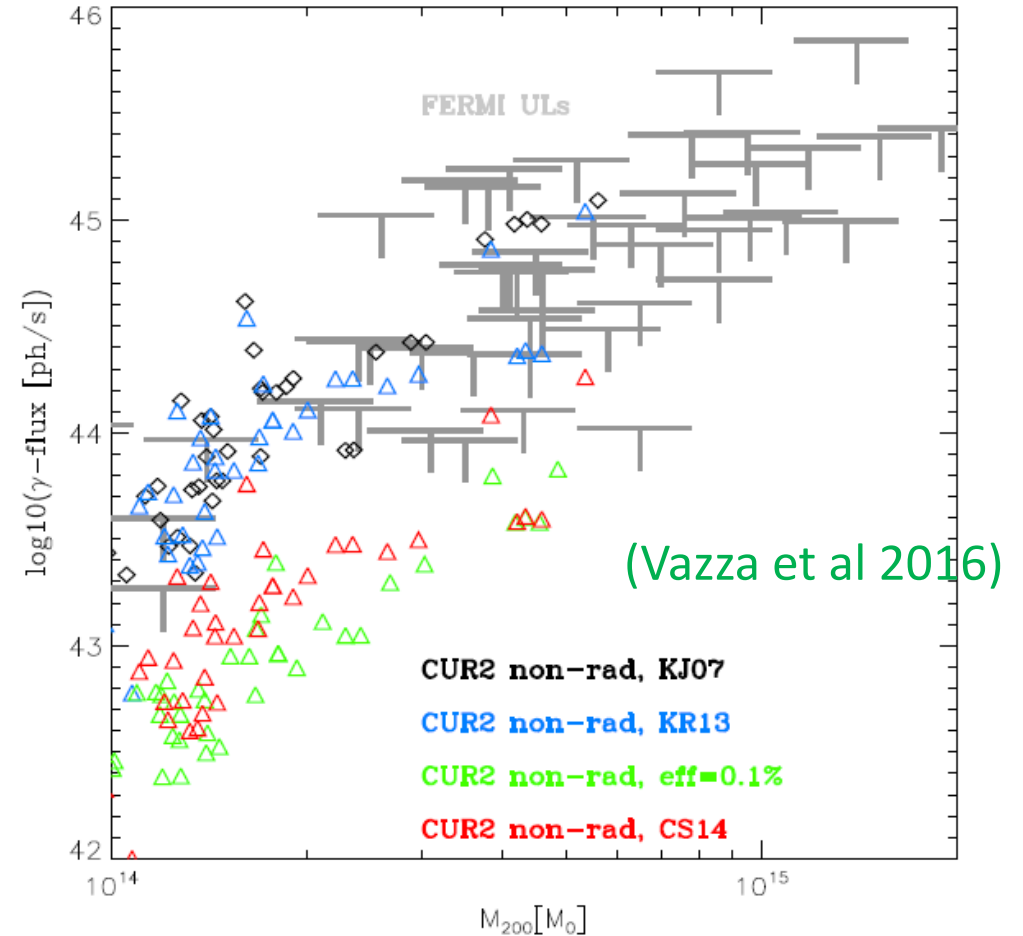


injection fraction $\xi \sim$ a few $\times 10^{-3}$

→ acceleration efficiency $\eta \sim$ a few %

→ consistent with hybrid sim results

ξ and η from simulation are too large!



to be compatible with Fermi upper limits, the CR proton acceleration eff. should be $\eta < 0.1\%$ for $2 < M < 5$

Summary

1. Shocks are abundant in and around galaxy clusters:
 - accretion accretion shocks: $10 < M_s < 10^2$: not detectable
 - intracluster shocks driven by mergers and chaotic flows: smaller M_s
 - **merger shocks with $M_s < \sim 3$** : detected as Radio relics/X-ray shocks
2. In high beta ICM, only **supercritical quasi-parallel shocks with $M_s > \sim 2.3$** may inject suprathermal protons to DSA and accelerate CR protons.
3. The injection fraction and DSA acceleration efficiency of CR protons are predicted to be too large in simulations.
 - need to understand the **long-term evolution of quasi-parallel shocks and proton acceleration**
4. **Electron acceleration at quasi-parallel shocks** in high beta ICM
 - see the next talk by Hyesung Kang

Thank you !